Molecular Biology of the Cell
Vol. 21, 2226–2240, July 1, 2010

Caveolin-1 Induces Formation of Membrane Tubules That Sense Actomyosin Tension and Are Inhibited by Polymerase I and Transcript Release Factor/Cavin-1

Prakhar Verma, Anne G. Ostermeyer-Fay, and Deborah A. Brown

Department of Biochemistry and Cell Biology, Stony Brook University, Stony Brook NY, 11794-5215

Submitted May 21, 2009; Revised April 6, 2010; Accepted April 21, 2010
Monitoring Editor: Robert G. Parton

Caveolin-1 and caveolae are often lost in cancer. We found that levels of caveolin-1 and polymerase I and transcript release factor (PTRF)/cavin-1 correlated closely in a panel of cancer and normal cells. Caveolin-1 reexpression in cancer cells lacking both proteins induced formation of long membrane tubules rarely seen in normal cells. PTRF/cavin-1 inhibited tubule formation when coexpressed with caveolin-1 in these cells, whereas suppression of PTRF/cavin-1 expression in cells that normally expressed both genes stimulated tubule formation by endogenous caveolin-1. Caveolin-1 tubules shared several features with previously described Rab8 tubules. Coexpressed Rab8 and caveolin-1 labeled the same tubules (as did EHD proteins), and synergized to promote tubule formation, whereas a dominant-interfering Rab8 mutant inhibited caveolin-1 tubule formation. Both overexpression and inhibition of dynamin-2 reduced the abundance of caveolin-1 tubules. Caveolin-1 reexpression in SK-BR-3 breast cancer cells also induced formation of short membrane tubules close to cortical actin filaments, which required actin filaments but not microtubules. Actomyosin-induced tension destabilized both long and short tubules; they often snapped and resolved to small vesicles. Actin filament depolymerization or myosin II inhibition reduced tension and stabilized tubules. These data demonstrate a new function for PTRF/cavin-1, a new functional interaction between caveolin-1 and Rab8 and that actomyosin interactions can induce tension on caveolin-1-containing membranes.

INTRODUCTION

Caveolae are 60- to 80-nm invaginations in the plasma membrane of mammalian cells that house proteins of the caveolin and cavin families (Parton and Simons, 2007; Bastiani *et al*., 2009). The caveolin protein family has three members. Caveolins-1 and -2 are coexpressed in a variety of cell types and can hetero-oligomerize with each other, whereas caveolin-3 is muscle specific (Parton and Simons, 2007). Caveolin-2 requires caveolin-1 for cell surface transport and caveolae formation. Caveolin-1 knockout mice have greatly reduced levels of caveolin-2 and lack caveolae outside muscle (Le Lay and Kurzchalia, 2005).

Four previously identified genes were recently shown to form the cavin family. Polymerase I and transcript release factor (PTRF)/cavin-1 was identified previously as polymerase I and transcript release factor (Hill *et al*., 2008; Liu *et al*., 2008). PTRF/cavin-1 and the other three members of the cavin family (serum deprivation protein response [SDPR; also called cavin-2]; serum deprivation response-related gene product that binds to C kinase [also called cavin-3]; and muscle-restricted coiled-coil protein [also called cavin-4]) can form a complex in the cytosol and on caveolae (Bastiani *et al*., 2009; Hansen *et al*., 2009). Membrane recruitment of this complex requires caveolin-1.

Caveolins, which have long been known to be required for caveolae formation (Parton and Simons, 2007), have an unusual topology. A central hydrophobic domain is flanked by hydrophilic N- and C-terminal domains that are both cytosolic. A similar structural motif allows reticulon proteins to deform the endoplasmic reticulum (ER) into tubules, suggesting that the hydrophobic hairpin in caveolins may form caveolae by the same mechanism (Shibata *et al*., 2008; Shnyrova *et al*., 2008). Recent results showed that PTRF/cavin-1 and SDPR/cavin-2 are also required for caveolae formation (Hill *et al*., 2008; Liu and Pilch, 2008; Hansen *et al*., 2009). In the absence of PTRF/cavin-1, caveolin-1 has a smooth, uniform distribution in the plasma membrane (Hill *et al*., 2008).

Interactions with the actin cytoskeleton normally immobilize caveolae in the plasma membrane (Pelkmans *et al*., 2002; Thomsen *et al*., 2002). However, caveolae can undergo endocytosis in response to stimuli including alterations of membrane lipid composition (Sharma *et al*., 2004) and binding of viruses such as simian virus 40 (Pelkmans *et al*., 2001). Internalized caveolae form caveolin-1–positive vesicles that move rapidly in a microtubule-dependent manner (Mundy *et al*., 2002; Tagawa *et al*., 2005) and fuse with caveolin-1–positive endocytic organelles called caveosomes (Pelkmans *et al*., 2001, 2004).

Several functions of caveolin-1 and caveolae may involve actin interactions. For example, caveolin-1 is required for directional migration of cultured fibroblasts (Grande-García *et al*., 2007; Sun *et al*., 2007). Cells lacking caveolin-1 migrate at normal speed but are defective in directional migration toward a chemotactic stimulus, as well as in directional persistency of random migration. Caveolin-1 was shown to

This article was published online ahead of print in *MBoC in Press* (http://www.molbiolcell.org/cgi/doi/10.1091/mbc.E09–05–0417) on April 28, 2010.

Address correspondence to: Deborah A. Brown (deborah.brown@sunysb.edu).

Abbreviations used: AF, AlexaFluor; CTxB, cholera toxin B subunit; LatA, latrunculin A; MBCD, methyl-β-cyclodextrin; Tf, transferrin.

affect directed cell motility through Src and RhoA (Grande-García *et al*., 2007). Caveolae also act in mechanosensation in endothelial cells and smooth muscle cells (Parton and Simons, 2007). In endothelial cells, exposure to shear stress increases the number of cell surface caveolae and increases cellular mechanosensitivity (Boyd *et al*., 2003; Rizzo *et al*., 2003). Furthermore, caveolin-1 is required for normal signaling in response to shear stress in vascular endothelial cells (Yu *et al*., 2006; Albinsson *et al*., 2008; Milovanova *et al*., 2008) and for normal stretch-induced activation of Akt in vascular smooth muscle cells (Sedding *et al*., 2005).

Caveolin-1 expression is reduced in several human tumors (Goetz *et al*., 2008; Quest *et al*., 2008; Perrone *et al*., 2009), suggesting that caveolin-1 may be a tumor suppressor (Williams and Lisanti, 2005). Consistent with this idea, reexpression of caveolin-1 in tumor cells can inhibit growth and invasiveness in vitro and slow tumor growth when breast cancer cells are inoculated into mouse mammary gland (Wiechen *et al*., 2001a,b; Fiucci *et al*., 2002; Sloan *et al*., 2004; Quest *et al*., 2008). However, the relationship between caveolin-1 and tumorigenesis is more complex than originally appreciated, and caveolin-1 is expressed at high levels in some tumors (Goetz *et al*., 2008; Quest *et al*., 2008). Differential caveolin-1 expression may relate to factors such as tissue type or tumor stage (Goetz *et al*., 2008). For example, breast cancers of the luminal subtype lose caveolin-1 expression, whereas those of the basal subtype and those that have undergone an epithelial–mesenchymal transition express the protein (Charafe-Jauffret *et al*., 2007; Finn *et al*., 2007).

To understand why caveolin-1 may be lost in cancer cells, we examined its localization after reexpression in several cancer cell lines. Caveolin-1 induced formation of membrane tubules when reexpressed in caveolin-1–negative cancer cells. These tubules are rare in normal cells (Parton *et al*., 1994; Mundy *et al*., 2002; Peters *et al*., 2003), suggesting that cancer cells lose a normal mechanism for inhibiting tubule formation when they lose caveolin-1 expression. Our results suggested that this mechanism involves PTRF/cavin-1. Caveolin-1 tubules interacted with both actin filaments and microtubules, as do caveolae and caveolin-1–positive vesicles in normal cells. Actin filament interactions exerted tension on the tubules.

Caveolin-1 tubules also contained Rab8 and EH domain-containing (EHD) proteins. The four mammalian EHD proteins act in both endocytosis and endocytic recycling (Naslavsky and Caplan, 2005). EHD proteins have some structural similarity to dynamins and can tubulate liposomes in vitro (Daumke *et al*., 2007). In cells, EHD proteins can localize to the same membrane tubules as Rab8 (Roland *et al*., 2007). Rab8 regulates plasma membrane-related trafficking events, including *trans*-Golgi network-to-plasma membrane transport (Huber *et al*., 1993; Peränen *et al*., 1996; Ang *et al*., 2003; Sahlender *et al*., 2005; Sato *et al*., 2007) and endocytic recycling (Ang *et al*., 2003; Linder *et al*., 2007; Roland *et al*., 2007), and also affects cell shape (Peränen *et al*., 1996; Hattula *et al*., 2006). Rab8 can also localize to Arf6-regulated membrane tubules (Hattula *et al*., 2006), where it can colocalize with EHD proteins (Roland *et al*., 2007). Our results revealed an unexpected relationship between Rab8/EHD tubules and tubules induced by caveolin-1.

MATERIALS AND METHODS

Cells and Transfection

Human breast cancer cell lines (SK-BR-3, MDA-MB-231, MDA-MB-468, and MCF-7), the melanoma line MDA-MB-435 (Lacroix, 2009), cervical carcinoma line HeLa, and untransformed NIH 3T3 fibroblasts and COS7 cells were obtained from American Type Culture Collection (Manassas, VA) or from U. Moll (Stony Brook University, Stony Brook, NY) and were cultured in DMEM with 10% iron-supplemented calf serum (JRH Biosciences, Lenexa, KS). T47D breast cancer cells (the gift of U. Moll) were grown with DMEM containing 10% fetal calf serum, 100 nM insulin, and 1 nM epidermal growth factor (EGF). MCF10A human mammary epithelial cells (the gift of M. Hayman, Stony Brook University) were grown in DMEM containing 5% horse serum, 20 ng/ml EGF, 100 ng/ml cholera toxin, 10 μg/ml insulin, and 0.5 μg/ml hydrocortisone. All media also contained penicillin/streptomycin. Cells were transiently transfected with Lipofectamine 2000 or Lipofectamine LTX (Invitrogen, Carlsbad, CA) according to the manufacturer's recommendation, by using 1 μg of each construct except where noted. Cells were examined 1–2 d after transfection.

Expression Constructs and Small Interfering RNA (siRNA)

Caveolin-1-green fluorescent protein (GFP) (encoding canine caveolin-1 fused at its C-terminal end to enhanced green fluorescent protein [EGFP]), in pEGFP-N1 (Clontech, Mountain View, CA) was the gift of D. Lublin (Washington University School of Medicine, St. Louis, MO). Caveolin-1-monomeric red fluorescent protein (mRFP), encoding mRFP fused to the C-terminal end of caveolin-1 (Pelkmans *et al*., 2004), was the gift of A. Helenius (ETH, Zurich, Switzerland.) Untagged human caveolin-1 (Mora *et al*., 1999) was the gift of E. Rodriguez-Boulan (Cornell University School of Medicine, New York, NY). EGFP-tagged constitutively active Rab5-Q79L (Volpicelli *et al*., 2001) was the gift of A. Levey (Emory University School of Medicine, Atlanta GA). Myc-EHD1 and myc-EHD3 plasmids were gifts of S. Caplan (University of Nebraska Medical Center, Omaha, NE) (Caplan *et al*., 2002). HA-EHD4 (Pincher) (Shao *et al*., 2002) was the gift of S. Halegoua (Stony Brook University). GFP-PH-PLCδ, the GFP-tagged pleckstrin homology (PH) domain of phospholipase C (PLC)δ (Várnai and Balla, 1998) was the gift of T. Balla (National Institutes of Health, Bethesda, MD). GFP-2x-FYVE, containing two copies of the FYVE domain of Hrs (Gillooly *et al*., 2000), was the gift of W. Maltese (Medical University of Ohio, Toledo, OH). Hemagglutinin (HA)-Arf6 and constitutively active HA-Arf6-Q67L (Hernández-Deviez *et al*., 2004) were the gifts of J. Casanova (University of Virginia, Charlottesville, VA). FLAG-PTRF/cavin-1 and PTRF/cavin-1-GFP were gifts of P. Pilch (Boston University, Boston, MA). GFP-Rab8, constitutively active GFP-Rab8-Q67L, and dominant-negative GFP-Rab8-T22N (Hattula *et al*., 2006) were gifts of J. Peränen (University of Helsinki, Helsinki, Finland). mCherry-α-tubulin (Dunn *et al*., 2008) was the gift of M. Peckham (University of Leeds, Leeds, United Kingdom). GFP-tagged nonmuscle myosin IIa and myosin IIb heavy chains, both in pEGFP-C3 (Wei and Adelstein, 2000), were from Addgene (www.addgene.org). HA-tagged dynamin-2 and dominant-negative dynamin-2K44A, both in pcDNA3, were gifts of S. Schmid (Scripps Institute, La Jolla, CA). Adipose triglyceride lipase (ATGL)-GFP (Smirnova *et al*., 2006) was the gift of C. Jackson (National Institutes of Health). ATGL-HA, with a C-terminal HA tag, was made by swapping in an HA tag for the GFP tag in ATGL-GFP, by using the QuickChange site-directed mutagenesis kit (Stratagene, La Jolla, CA). The sequence of the sense primer: TACCCATATGACGTCCCAGATTACGCGTAA. HA-tagged intersectin (Mohney *et al*., 2003) was the gift of J. O'Bryan (University of Illinois College of Medicine, Chicago, IL). pGW1HA-spartin (Bakowska *et al*., 2007) was the gift of C. Blackstone (National Institutes of Health). pBC12/PLAP, encoding placental alkaline phosphatase (PLAP), has been described previously (Berger *et al*., 1987). A recombinant adenovirus expressing human caveolin-1 was from Vector Biolabs (Philadelphia, PA). The virus was expanded in human embryonic kidney-293T cells and purified following recommendations of the supplier. siRNA duplex constructs to knock down Rab8a and PTRF/cavin-1, made using Stealth RNA interference (RNAi) siRNA technology, were from Invitrogen. The targeted sequence for Rab8a knockdown, chosen based on previous work (Schuck *et al*., 2004; Hattula *et al*., 2006), was GACAAGAGACAAGTTTCCAAGGAAC. The targeted sequences for PTRF/cavin-1 knockdown were GCCGCAACTTTAAAGTCATGATCTA (#1), AGGAGTCCCGCGCAGAGCGTATCAA (#2), and CCGGCCAAACTGAGCATCAGCAAAT (#3). The Medium GC Stealth RNAi siRNA Duplex (12935-300; Invitrogen) was used as a control for both knockdown experiments. For Rab8a knockdown, HeLa cells grown on coverslips (for fluorescence analysis of caveolin-1-GFP tubule formation) or in 35-mm dishes (for assessment of Rab8a knockdown by Western blotting) were transfected with siRNA duplexes using Lipofectamine 2000, and then with caveolin-1-GFP 24 h later, and harvested 24 or 48 h after that. For PTRF/cavin-1 knockdown, MDA-MB-231 cells were grown and transfected with siRNA duplexes as for HeLa cells and grown 48 or 72 h before harvest for analysis of PTRF/cavin-1 expression by Western blotting, or of endogenous caveolin-1 localization by immunofluorescence microscopy.

Antibodies, Fluorescent Compounds, and Other Reagents

Mouse anti-heat-shock protein (Hsp)70 and anti-Hsp90 antibodies were from Santa Cruz Biotechnology (Santa Cruz, CA). Rabbit anti-caveolin-1, mouse anti-Rab8, mouse anti-PTRF, and mouse anti-early endosomal antigen (EEA)1 antibodies were from Transduction Laboratories, BD Biosciences (San Jose, CA). Mouse anti-myc tag antibodies were from Invitrogen. Rabbit anti-HA tag antibodies were from Sigma-Aldrich (St. Louis, MO). Secondary antibod-

ies: AlexaFluor (AF)-488 and AF-594-conjugated goat anti-mouse and goat anti-rabbit immunoglobulin (Ig)G were from Invitrogen. Rhodamine was conjugated to human transferrin (Tf) using *N*-hydroxysuccinimide-rhodamine (Pierce Chemical, Rockford, IL), by the procedure recommended by Pierce Chemical. AF-594-phalloidin, AF-594-cholera toxin B subunit (CTxB), Texas Red-Tf, and fluoro-ruby dextran (10,000 mol. wt.) were from Invitrogen. Sources for other reagents were as follows: latrunculin A (LatA) (used at 3–5 μM and treating cells for 10–30 min) was from Enzo Life Sciences International (Plymouth Meeting, PA), dynasore was from ChemBridge (San Diego, CA), and blebbistatin was from Calbiochem, EMD Biosciences (San Diego, CA). Protein assay reagents were from Bio-Rad Laboratories (Hercules, CA). All other reagents were from Sigma-Aldrich.

Fluorescence Microscopy

Cells were grown and processed for fluorescence microscopy as described previously (Barr *et al*., 2008). Images of fixed cells were captured and processed either by wide-field epifluorescence microscopy, by using an Axioskop 2 microscope (Carl Zeiss, Jena, Germany) with a 100× objective (numerical aperture 1.3) (Ostermeyer *et al*., 2001, 2004) or by confocal microscopy, using an inverted Axiovert 200 M microscope (Carl Zeiss) with a two-photon laser scanning confocal system and a 100× oil immersion objective, processing images with LSM software (Carl Zeiss). When necessary, images were further processed using Photoshop (Adobe Systems, Mountain View, CA), adjusting intensity (levels), contrast, and/or brightness for optimal viewing. Each channel was adjusted separately, but each adjustment was applied to the whole field. The fraction of transfected cells in which caveolin-1 was present in tubules was determined by wide-field epifluorescence microscopy. Cells were scored positive if they contained at least two tubules, each at least 5 μm long. At least 150 cells on each slide were counted.

To compare caveolin-1 expression levels in different cell types, NIH 3T3 and SK-BR-3 cells were grown in parallel on coverslips, and caveolin-1 was expressed in SK-BR-3 cells. Cells were fixed, permeabilized, and incubated in parallel with anti-caveolin-1 antibodies and AF-594-goat anti-rabbit secondary antibodies. Mean fluorescence in 35–40 randomly selected NIH 3T3 cells, and the same number of transfected SK-BR-3 cells that contained long caveolin-1–positive tubules, was measured using the confocal microscope described above, by using LSM software (Carl Zeiss). Acquisition parameters were the same for all cells, and images were not processed.

Three-dimensional (3D) reconstruction of fixed cells was performed using an Axiovert 200 deconvolution microscope (Carl Zeiss) equipped with an Axiocam digital camera (Carl Zeiss). To acquire z-stacks, 25–35 serial images were recorded at 350-nm intervals along the *z*-axis by using a 100× oil immersion objective. Out-of-plane fluorescence was removed by deconvolution using the inverse filter algorithm. Images were further processed to increase signal intensity using Axiovision software, version 4.7.1. Live cell microscopy was performed on the same deconvolution microscope. SK-BR-3 cells were seeded on 35-mm glass-bottomed dishes (MatTek, Ashland, MA). Cells were transfected as described above and were imaged live after 1–2 d. Dishes were inserted in a chamber on the microscope stage that was maintained at 37°C in a 5% CO_2 atmosphere. All images were acquired using a 100× oil immersion objective. Images were acquired at frame intervals of 10–15 s with the exposure time calculated automatically. The images were processed to make movies, and tubule length measured where appropriate, by using Axiovision software.

For internalization experiments, AF-594-CTxB (0.5 μg/ml), fluoro-ruby dextran (1 mg/ml), or rhodamine- or Texas Red-Tf (35 μg/ml) were added to the growth medium for times indicated in figure legends. Where indicated, 10 μM nocodazole, 3–5 μM LatA, 80 μM dynasore, or 10 mM methyl-β-cyclodextrin (MBCD) was added to cells for times indicated in figure legends. For energy depletion, cells were incubated for 30 min in phosphate-buffered saline (Barr *et al*., 2008) containing 20 mM 2-deoxy-D-glucose and 10 mM sodium azide. Control cells were incubated in phosphate-buffered saline containing 20 mM D-glucose.

Other Methods

SDS-polyacrylamide gel electrophoresis (PAGE), transfer to polyvinylidene difluoride, Western blotting, and detection of bands on film by enhanced chemiluminescence were performed as described previously (Schroeder *et al*., 1998). Quantitation of scanned bands was performed using ImageJ (National Institutes of Health).

RESULTS

Localization of Caveolin-1 Expressed in SK-BR-3 Breast Cancer Cells

It is not known why caveolin-1 is lost in many cancer cells. We reasoned that aberrant localization of reexpressed caveolin-1 in such cells might provide clues. In normal cells, caveolin-1 is localized to caveolae, caveosomes, and small vesicles that move between the plasma membrane and the cell interior in a microtubule-dependent manner (Pelkmans *et al*., 2001; Mundy *et al*., 2002; McMahon *et al*., 2009). Small pools are present in early endosomes (Pelkmans *et al*., 2001) and in the Golgi in some cell types (Denker *et al*., 1996; Ren *et al*., 2004). We expressed caveolin-1 in SK-BR-3 breast cancer cells, which lack caveolin-1 and caveolae (Hommelgaard *et al*., 2004). To facilitate live-cell imaging, most experiments were done with caveolin-1-GFP or caveolin-1-red fluorescent protein (RFP). Both proteins have been show to localize in the same manner as endogenous caveolin-1 in normal cells (Pelkmans *et al*., 2001; Mundy *et al*., 2002).

Reexpressed caveolin-1-GFP (Figure 1A) and untagged caveolin-1 (Figure 1B) had similar localization patterns in SK-BR-3 cells. Both were present in small puncta on and near the plasma membrane, in larger puncta throughout the cytosol, and sometimes in amorphous perinuclear structures. Many of the cytosolic puncta were probably caveosomes (Pelkmans *et al*., 2001), although the protein was also easily detectable in early endosomes. As in other cells (Pelkmans *et al*., 2004), coexpression of caveolin-1-RFP with constitutively active GFP-Rab5-Q79L often increased the amount of caveolin-1-RFP in endosomes (Figure 1C). High Rab5 function may slow exit of caveolin-1 from early endosomes, allowing it to accumulate there.

Reexpressed caveolin-1 was sometimes present in membrane tubules in SK-BR-3 cells (Figure 1, A–C). These tubules fell into two classes, which we termed long and short. Caveolin-1–positive long tubules have been reported previously (Parton *et al*., 1994; Mundy *et al*., 2002; Peters *et al*., 2003), but they are rare, and detailed studies of their structure have not been possible. Because long tubules were relatively abundant in SK-BR-3 cells, we were able to examine them more carefully. We discuss these results first and then describe short tubules.

Caveolin-1 Stimulates Formation of Endocytic Tubules with Characteristics of Plasma Membrane but Not Early Endosomes

Caveolin-1–positive long tubules were often 10–30 μm long, and sometimes up to 50 μm, and often branched (Figure 1A; also see Supplemental Figure 1 and Supplemental Movie 1). Long tubules were seen most clearly in well-spread cells. Such cells were often 60–80 μm in diameter, but only ~5 μm high (Supplemental Figure 1). 3D reconstruction showed that long tubules ran roughly parallel to the substrate, as dictated by cell shape, but were not precisely aligned with each other and were not obviously concentrated at any particular height in the cell (Supplemental Figure 1 and Supplemental Movie 1.)

To determine whether the long tubules were derived from the plasma membrane, we determined whether they could be labeled with CTxB, added to the media of living cells. Although the tubules were rarely labeled after 2 min of CTxB uptake (data not shown), they almost all contained internalized CTxB after 10 min, showing that most were endocytic (Figure 1D). CTxB was very rarely (<1% of cells) seen in long tubules in untransfected SK-BR-3 cells, and these were never abundant (data not shown). Thus, caveolin-1-GFP stimulated formation of plasma membrane-derived tubules in SK-BR-3 cells.

Phosphatidylinositol 4,5-bisphosphate [PI(4,5)P_2] is abundant in the plasma membrane but is normally cleaved by phosphatases soon after internalization (Cremona *et al*., 1999), and it is not present at high levels in early endosomes or other organelles. Caveolin-1–positive tubules could be labeled with the PI(4,5)P_2 probe GFP-PH-PLCδ, showing that they retained this plasma membrane marker (Figure 1E).

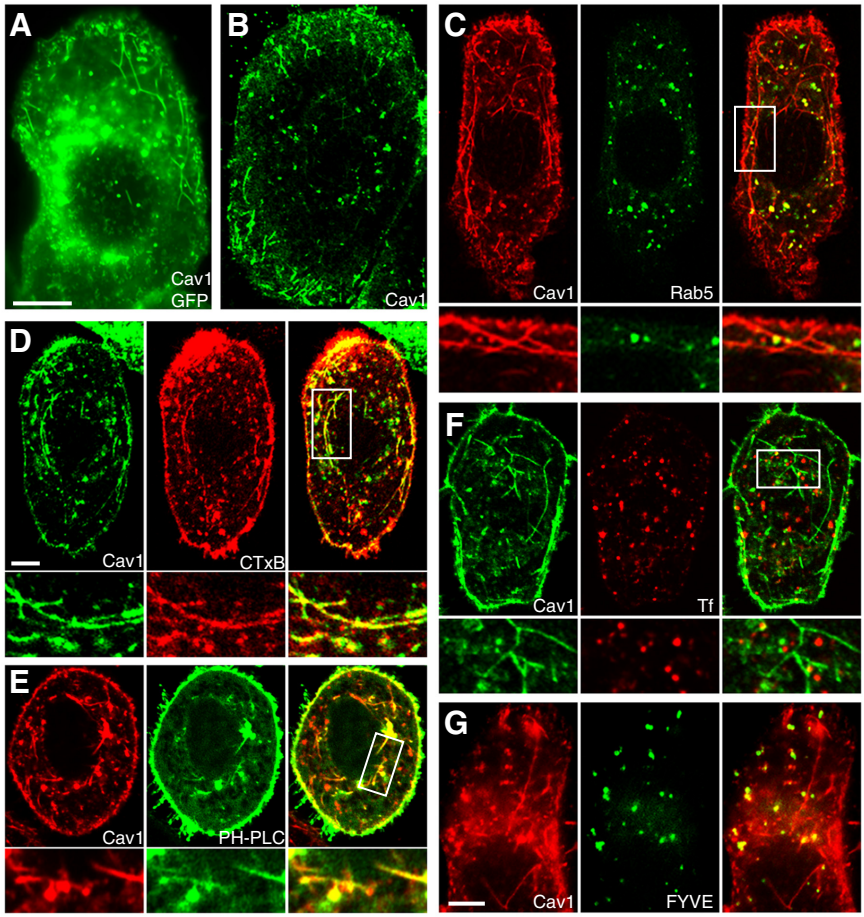

Figure 1. Caveolin-1 induces plasma membrane-derived endocytic tubules, not linked to early endosomes, in SK-BR-3 cells. (A and B) Caveolin-1-GFP (A) or untagged caveolin-1 (B) was expressed in SK-BR-3 cells and examined by fluorescence microscopy, detecting untagged caveolin-1 with anti-caveolin-1 antibodies. (C) Constitutively active GFP-Rab5-Q79L (middle) and caveolin-1-RFP (left) were coexpressed in SK-BR-3 cells. (C–F) High-magnification views of the boxed region in the merged image (right) are shown beneath each panel. (D) AF-594-CTxB (middle) was added to SK-BR-3 cells expressing caveolin-1-GFP (left) for 10 min before fixation and examination by fluorescence microscopy. (E) GFP-PH-PLCδ (middle) and caveolin-1-RFP (left) were coexpressed in SK-BR-3 cells, which were fixed and visualized by fluorescence microscopy. (F) SK-BR-3 cells expressing caveolin-1-GFP (left) were incubated with 35 μg/ml rhodamine-Tf (middle) for 10 min, 37°C, before fixation. (G) Caveolin-1-RFP (left) and GFP-2x-FYVE (middle) were coexpressed in SK-BR-3 cells before fixation and visualization by fluorescence microscopy. Bar in A (applies to A and B), 10 μm. Bars in C (applies to C–F) and G, 5 μm.

Soon after internalization, vesicles internalized by clathrin-mediated endocytosis and also by several clathrin-independent pathways are delivered to Rab5/EEA1-positive early endosomes, merging cargo internalized by clathrin-dependent and clathrin-independent pathways (Naslavsky *et al.*, 2003; Sharma *et al.*, 2003; Kalia *et al.*, 2006; Barr *et al.*, 2008). By contrast, caveolin-1 tubules did not contain GFP-Rab5-Q79L (Figure 1C) or EEA1 (data not shown), and they did not contain internalized Tf (Figure 1F), or the early endosome-specific phosphatidylinositol-3-phosphate [PI(3)P], because they were not labeled by the PI(3)P probe GFP-2x-FYVE (Figure 1G). Thus, caveolin-1-GFP tubules do not acquire characteristics of early endosomes. Furthermore, we did not see contact between caveolin-1 tubules and EEA1-positive endosomes, suggesting that they do not deliver cargo to endosomes.

Caveolin-1 Long Tubules Require Microtubules but Not Actin Filaments

Caveolin-1–positive tubules in CHO cells are microtubule dependent (Mundy *et al.*, 2002). Similarly, microtubule disruption with nocodazole abolished caveolin-1-GFP long tubules in SK-BR-3 cells (data not shown). Long tubules rarely colocalized with microtubules (visualized with coexpressed mCherry-α-tubulin; Figure 2A). This suggested that microtubule-interacting proteins were not distributed along the length of the membrane tubules. Nevertheless, interactions with microtubules probably determine the position and distribution of long tubules in cells.

To determine whether long tubules required the actin cytoskeleton, we depolymerized actin filaments with LatA. LatA did not disrupt, and in fact enhanced long tubule accumulation: abundant tubules were seen in 40–60% of transfected SK-BR-3 cells after LatA treatment but only 10–20% of untreated cells. In further studies, we used LatA as a convenient tool to increase tubule number, to get a clearer picture of whether other treatments administered at the same time affected tubule formation. As in untreated cells, almost all caveolin-1-GFP long tubules could be labeled by CTxB in 10 min in LatA-treated cells (Figure 2B). However, additional results, described later, showed that caveolin-1 long tubules interacted with and were affected by the actin cytoskeleton.

Caveolin-1-GFP–positive Long Tubules are More Common in Cancer Cells That Have Lost Endogenous Caveolin-1 Expression

To determine whether tubular localization was unusually common in SK-BR-3 cells, we examined several other cell lines. COS7, NIH 3T3, and MCF10A (mammary epithelial cells) are not transformed, whereas MCF7, SK-BR-3, T47D, and MDA-MB-468 are breast cancer cell lines of the luminal subtype (Finn *et al.*, 2007). MDA-MB-231 breast cancer cells have undergone an epithelial-mesenchymal transition (EMT) (Finn *et al.*, 2007). MDA-MB-435, previously thought to be post-EMT breast cancer cells, were recently shown to be melanoma cells (Lacroix, 2009). HeLa cells are from a cervical carcinoma. Tubules positive for transfected caveolin-1-GFP were seen in all cell lines, but the frequency varied widely (Figure 3A). We next examined caveolin-1 levels in the different cell lines (Figure 3B). Consistent with previous

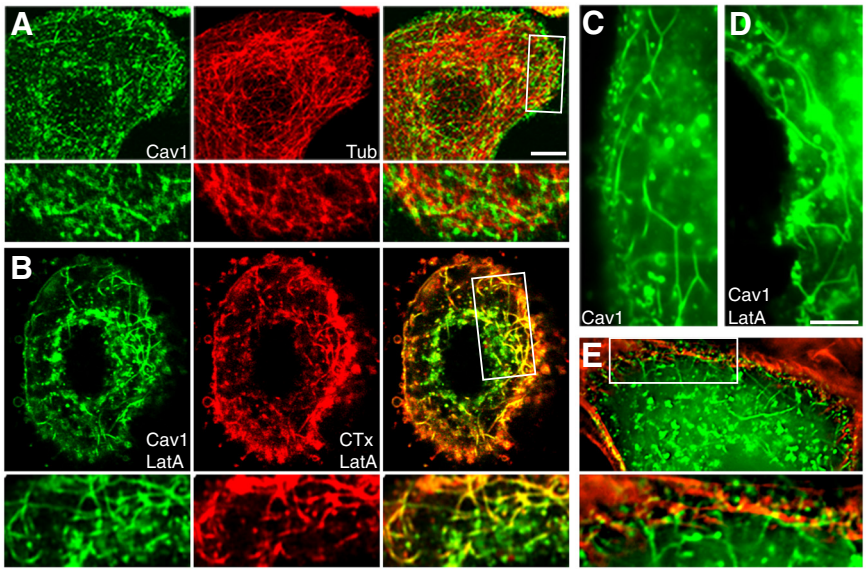

Figure 2. Interactions of caveolin-1 tubules with actin and microtubule cytoskeletons in SK-BR-3 cells. (A) Cells expressing caveolin-1-GFP (left) and mCherry-α-tubulin (middle) were visualized by fluorescence microscopy. Caveolin-1-GFP tubules rarely colocalized with microtubules. (A, B, and E) High-magnification views of the boxed region in the merged images are shown beneath each panel. (B) Cells expressing caveolin-1-GFP (left) were treated with 5 μM LatA for 30 min. AF-594-CTxB (middle) was added for the last 10 min, and cells were fixed and examined by fluorescence microscopy. (C and D) Morphology of tubules in caveolin-1-GFP–expressing control (C) and LatA-treated (D) cells. (E) A cell expressing caveolin-1-GFP was fixed, permeabilized, and incubated with AF-594-phalloidin to label actin filaments. Short tubules and puncta associated with actin filaments under the plasma membrane, whereas long tubules extended into the cell from the actin-rich subcortical region. An enlarged view of the boxed region is shown beneath the panel. Bars, 5 μm (bar in A applies to A and B; bar in D applies to C-E).

results, caveolin-1 was expressed in untransformed cells and in the post-EMT breast cancer cells, but expression was low or undetectable in luminal subtype breast cancer cells (Finn *et al*., 2007). Caveolin-1 expression was also greatly reduced in MDA-MB-435 and HeLa cells, despite the fact that the protein was easily detectable by immunofluorescence microscopy (data not shown). Tubular localization of caveolin-1-GFP correlated inversely with endogenous caveolin-1 expression: tubules were abundant in cells with low or undetectable caveolin-1, and rare in cells with abundant caveolin-1. This suggested that when cancer cells lost caveolin-1 expression, they also lost the ability to limit caveolin-1–induced membrane tubulation.

These results suggested that the ability of caveolin-1 to form tubules did not result simply from overexpression. As a further test of this idea, we compared caveolin-1-GFP levels in transfected SK-BR-3 cells that contained tubules, with levels of endogenous caveolin-1 in NIH 3T3 cells, by quantitative confocal microscopy (Supplemental Figure 2). As expected, caveolin-1 expression levels were more heterogeneous in transfected SK-BR-3 cells than in NIH 3T3 cells. Tubules were rare in very high-expressing SK-BR-3 cells, which often accumulated caveolin-1 in the ER or in perinuclear structures. Although many tubule-containing SK-BR-3 cells contained more caveolin-1 than did NIH 3T3 cells, many others contained about the same amount (Supplemental Figure 2). This suggested that tubule formation does not require superphysiological levels of caveolin-1.

PTRF/Cavin-1 Is Expressed Coordinately with Caveolin-1 and Inhibits Caveolin-1–induced Tubule Formation

Expression levels of PTRF/cavin-1 and caveolin-1 are coordinated in many tissues (Hill *et al*., 2008; Liu *et al*., 2008; Bastiani *et al*., 2009) and may be interregulated: levels of each protein are reduced in mice lacking the other gene (Hill *et al*., 2008; Liu *et al*., 2008). Nevertheless, at least one prostate cancer cell line is known to express caveolin-1 but not PTRF/cavin-1 (Hill *et al*., 2008; Bastiani *et al*., 2009). We found that with one exception, PTRF/cavin-1 expression correlated closely with caveolin-1 expression in our panel of cell lines (Figure 3B). Thus, PTRF/cavin-1 expression, as well as that of caveolin-1, correlated inversely with the ability of reexpressed caveolin-1 to form membrane tubules. COS7 cells were an exception: for unknown reasons, PTRF/cavin-1 was undetectable on Western blots, although caveolin-1 was expressed (Figure 3B).

We next asked whether exogenous expression of either caveolin-1 or cavin-1 in SK-BR-3 cells induced endogenous expression of the other gene. We first expressed either PTRF/cavin-1-GFP or soluble GFP in these cells for 3 d, and then we analyzed cells for expression of endogenous caveolin-1 by Western blotting (Figure 3C). Caveolin-1 was not detected in PTRF/cavin-1–transfected cells, despite efficient expression of PTRF/cavin-1-GFP. By contrast, endogenous caveolin-1 in the same amount of NIH 3T3 cell lysate was easily detectable (Figure 3C). Caveolin-1 was undetectable by immunofluorescence even in transfected cells that expressed the highest levels of PTRF/cavin-1 (data not shown).

To determine whether caveolin-1 reexpression induced endogenous PTRF/cavin-1 expression, SK-BR-3 cells were infected with a recombinant adenovirus expressing caveolin-1. Immunofluorescence analysis showed that >90% of infected cells expressed caveolin-1 by 24 h after infection. Expression remained high for at least 4 d (Figure 3D; data not shown). Nevertheless, although endogenous PTRF/cavin-1 was easily detectable in NIH 3T3 cells, it was not seen in adenovirus/caveolin-1 infected SK-BR-3 cells (Figure 3D). We conclude that short-term reexpression of caveolin-1 or PTRF/cavin-1 in SK-BR-3 cells does not induce expression of the other gene.

To determine whether PTRF/cavin-1 affected caveolin-1–induced tubule formation, we coexpressed caveolin-1-GFP and FLAG-PTRF/cavin-1 in SK-BR-3 cells. As shown previously (Hill *et al*., 2008), FLAG-PTRF/cavin-1 colocalized closely with GFP-caveolin-1 in puncta near the plasma membrane but not with GFP-caveolin-1 in perinuclear structures (Figure 4, A and B). When expressed alone in SK-BR-3 cells, FLAG-PTRF/cavin-1 had a predominantly cytosolic localization, although some plasma membrane-associated puncta were detected, and the protein was never present on membrane tubules (data not shown). Coexpression with FLAG-PTRF/cavin-1 greatly reduced the frequency of caveolin-1 tubules, both with and without LatA treatment (Figure 4G,

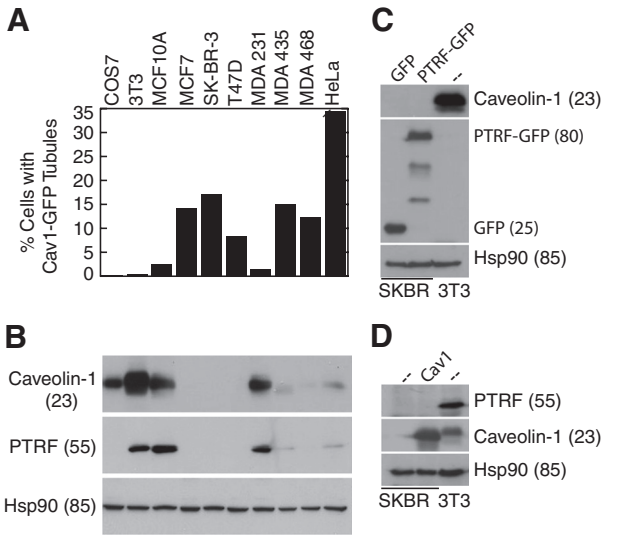

Figure 3. Caveolin-1-GFP tubules correlate with loss of endogenous caveolin-1 and PTRF/cavin-1; forced expression of PTRF/cavin-1 or caveolin-1 does not induce endogenous expression of the other gene in SK-BR-3 cells. (A) Caveolin-1-GFP was expressed in COS7, NIH 3T3, MCF-10A, MCF-7, SK-BR-3, T47D, MDA-MB-231, MDA-MB-435, MDA-MB-468, and HeLa cells. The percentage of transfected cells in which caveolin-1 was detected in tubules by fluorescence microscopy is indicated (average of at least 2 experiments that varied by <15%, counting at least 150 transfected cells in each). (B) Lysates of the cells listed in A were analyzed by SDS-PAGE and Western blotting, detecting caveolin-1, PTRF/cavin-1, and Hsp90 as a loading control. Cell line labels in A also refer to the corresponding bands in B. (C) SK-BR-3 cells (first 2 lanes) were transfected with GFP or PTRF/cavin-1-GFP as indicated (top of blot) and grown for 3 d before harvest. Lysates of these cells and of untransfected NIH 3T3 cells (third lane) containing 25 μg of protein were subjected to SDS-PAGE and transfer to polyvinylidene difluoride (PVDF). The blot was probed sequentially with anti-caveolin-1, anti-GFP, and anti-Hsp90, stripping between probings. (D) SK-BR-3 cells (first 2 lanes) were infected with caveolin-1-expressing adenovirus as indicated (top of blot), or left uninfected, and grown for 4 d before harvest. Lysates of these cells and of uninfected NIH 3T3 cells (third lane) containing 25 μg of protein were subjected to SDS-PAGE and transfer to PVDF. The blot was probed sequentially with anti-PTRF/cavin-1, anti-caveolin-1, and anti-Hsp90, stripping between probings. (B–D) Molecular masses (in parentheses) are in kilodaltons.

top half of graph). In most cotransfected cells, caveolin-1-GFP had a primarily punctate localization (Figure 4A). However, FLAG-PTRF/cavin-1 colocalized with caveolin-1 on the rare tubules present (Figure 4B). PTRF/cavin-1-GFP behaved in a similar manner to FLAG-PTRF/cavin-1, except that plasma membrane puncta were rarely seen when PTRF/cavin-1-GFP was expressed without caveolin-1 (data not shown).

To determine whether PTRF/cavin-1 inhibited tubule formation by endogenous caveolin-1, we suppressed its expression with siRNA in MDA-MB-231 cells, and then examined the localization of endogenous caveolin-1. Three PTRF/cavin-1–targeted siRNA duplexes gave similar levels of suppression (Supplemental Figure S3). In control cells, caveolin-1 was mostly localized in caveolae and sometimes in larger vacuole-like structures (Figure 4C). Caveolin-1 had a similar localization in PTRF/cavin-1–suppressed cells, except that it was also present in long tubules in ~10% of the cells (Figure 4, D, E, and H). (Caveolin-1–positive tubules were occasionally seen in control cells. However, unlike tubules in PTRF/cavin-1–suppressed cells, they were never longer than ~5 μm, and no more than 1 or 2 tubules were seen per cell.) Growth for three instead of 2 d after transfection with PTRF/cavin-1–targeted siRNA duplexes did not increase the fraction of cells with tubules.

Together, these results showed that reexpressed caveolin-1 did not require PTRF/cavin-1 to deform the plasma membrane into tubules but that PTRF/cavin-1 limited the ability of caveolin-1 to form tubules. The loss of PTRF/cavin-1 in cancer cells is likely to explain the increased tendency of reexpressed caveolin-1 to form tubules in these cells.

Caveolin-1 Tubules Require Membrane Cholesterol

Cholesterol depletion or sequestration induces dramatic flattening of caveolae within a few minutes (Rothberg *et al*., 1992; Hailstones *et al*., 1998). To determine the effect of cholesterol on caveolin-1-GFP dynamics and tubule formation in SK-BR-3 cells, we depleted cholesterol with MBCD (Kilsdonk *et al*., 1995). MBCD greatly reduced the frequency of caveolin-1 tubules (Figure 5H), and caveolin-1-GFP often had a smooth appearance in the plasma membrane (Figure 5A).

SK-BR-3 cells sometimes contain large plasma membrane-derived vacuoles (our unpublished data). These are likely to be macropinosomes, formed by constitutive plasma membrane ruffling that occurs in these cells. Caveolin-1-GFP–positive vacuoles were especially prominent in MBCD-treated cells and were seen in most cells after drug treatment (Figure 5, A–C). At least some vacuoles could be labeled with fluorescent dextran, added to media as a marker of fluid phase endocytosis, after 5 min (Figure 5, A and B). This occurred despite the fact that constitutive internalization of dextran in small endocytic puncta was greatly inhibited by MBCD (data not shown), consistent with a general cholesterol requirement for clathrin-independent pinocytic pathways (Naslavsky *et al*., 2004). Together, these results suggest that at least some of the vacuoles that accumulated after MBCD treatment were macropinosomes. Some vacuoles may also have been recycling structures: they occasionally moved slowly toward the plasma membrane and fused with it (Supplemental Movie 2; selected frames shown in Figure 5C).

Although tubules disappeared and vacuoles became more prominent after MBCD treatment, we saw no indication that MBCD induced a switch from tubule to vacuole formation. In fact, in control cells, although vacuole formation was more variable than in MBCD-treated cells, we often saw vacuoles and tubules in the same cells. Tubules were very rare when LatA was added after MBCD pretreatment but were more frequent when cells were treated with LatA before addition of MBCD (Figure 5, D–H). This suggested that cholesterol depletion blocked the formation of new tubules, even in the presence of LatA, but that preformed tubules that accumulated in the presence of LatA were at least somewhat resistant to disruption by MBCD.

Caveolin-1 Long Tubules Require Dynamin Function but Are Inhibited by Dynamin-2 Overexpression

Shiga toxin induces formation of plasma membrane tubules, in a manner that is enhanced by energy depletion (Römer *et al*., 2007). Reduction of dynamin function also stimulates Shiga toxin tubule formation, and tubules are labeled by dominant-negative dynamin (Römer *et al*., 2007). These results suggested that dynamins reduce accumulation of Shiga toxin tubules by cleaving tubules into vesicles, and energy

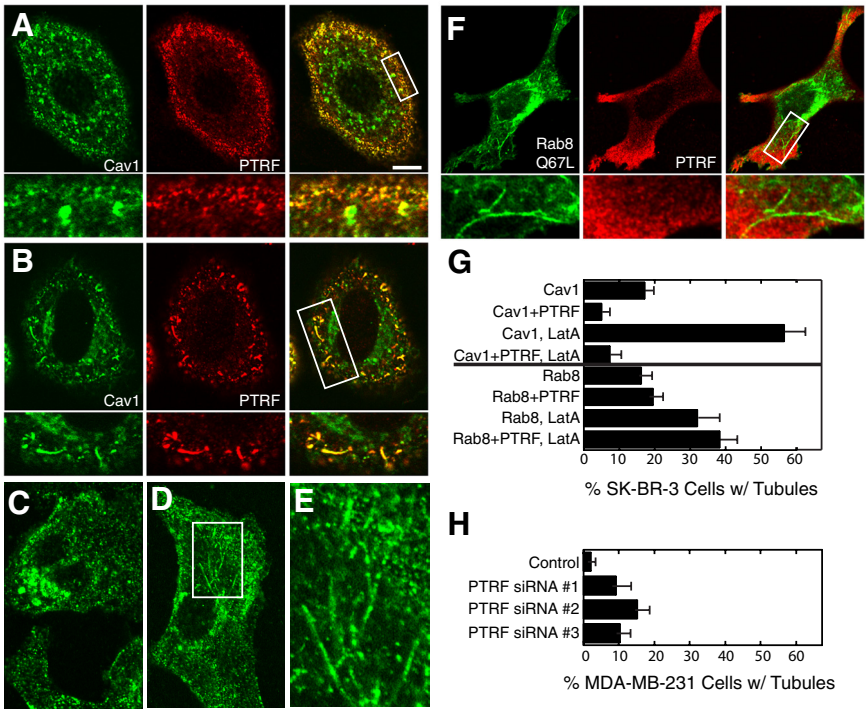

Figure 4. PTRF/cavin-1 reduces caveolin-1 tubule frequency and associates with residual tubules, but does not associate with or affect Rab8 tubules. (A, B, and F) SK-BR-3 cells expressing FLAG-PTRF/cavin-1 (PTRF; center panels) together with caveolin-1-GFP (A and B; left) or GFP-Rab8-Q67L (F; left) were processed for immunofluorescence microscopy, detecting FLAG-PTRF/cavin-1 with anti-FLAG antibodies. High-magnification views of the boxed region in the merged image (right) are shown beneath each panel. Panel A shows a typical cell with no tubules; B shows an unusual cell containing tubules, on which caveolin-1-GFP and FLAG-PTRF/cavin-1 colocalized. (C–E) MDA-MB-231 cells transfected with control siRNA (C) or PTRF/cavin-1-targeted siRNA duplex #1 (D and E) were grown 2 d after transfection and processed for immunofluorescence microscopy, detecting caveolin-1 with specific antibodies. (E) High-magnification image of the region boxed in D. Bar, 5 μm. (G) SK-BR-3 cells expressing GFP-caveolin-1 (Cav1) or GFP-Rab8Q67L (Rab8), with or without FLAG-PTRF/cavin-1 (PTRF), with or without 10-min LatA treatment were processed for immunofluorescence microscopy. The percentage of transfected cells containing long tubules positive for caveolin-1-GFP or GFP-Rab8Q67L as appropriate was determined. The mean ± SEM of at least three experiments (counting at least 150 cells on each slide) is shown. (H) MDA-MB-231 cells transfected with control or PTRF/cavin-1 siRNA duplexes as indicated were processed as described in C–E, and the percentage of cells containing long tubules positive for caveolin-1 was determined as described in G.

depletion enhances tubule formation at least in part by inhibiting dynamin function (Römer *et al.*, 2007).

We next determined whether caveolin-1 tubules in SK-BR-3 cells were regulated in a similar manner. As for Shiga toxin tubules, energy depletion enhanced caveolin-1 tubule accumulation (Figure 6A, top). Overexpression of HA-dynamin-2 also greatly reduced caveolin-1 tubule frequency, suggesting that dynamin-2 may cleave tubules to vesicles. However, in contrast to Shiga toxin, inhibition of dynamin function by dynasore (Macia *et al.*, 2006) or by overexpression of dominant-negative HA-dynamin-2-K44A also reduced the frequency of caveolin-1 tubules (Figure 6A, top). Inhibition of tubule accumulation by both wild-type and dominant-negative dynamins was most dramatic in LatA-treated cells (Figure 6A, bottom). To ensure the specificity of these effects, caveolin-1-GFP was coexpressed with four other constructs that were not expected to affect tubule formation. PLAP, HA-ATGL (a lipid droplet lipase; Smirnova *et al.*, 2006), HA-intersectin (ITSN; involved in endocytosis; Mohney *et al.*, 2003), and HA-spartin (implicated in endocytosis and lipid droplet dynamics; Bakowska *et al.*, 2007; Eastman *et al.*, 2009) were all efficiently expressed, as judged by immunofluorescence microscopy (data not shown), but none inhibited caveolin-1 tubule accumulation in cotransfected LatA-treated SK-BR-3 cells (Figure 6A, bottom). Tubule frequency in all cases was similar to that in LatA-treated cells expressing caveolin-1-GFP alone (Figures 4–7). As expected, HA-dynamin-2-K44A inhibited Tf internalization, whereas wild-type HA-dynamin-2 did not (Figure 6B). (This assay probably underestimated the inhibitory effect of dominant negative dynamin-2 on Tf internalization, because cells containing any visible internalized Tf were scored as positive for internalization.)

Caveolin-1-GFP and Rab8 Synergize to Form Tubules That Are Regulated by Rab8 and Arf6 and Recruit EHD Proteins

EHD proteins can localize to microtubule-dependent membrane tubules (Caplan *et al.*, 2002; Galperin *et al.*, 2002; George *et al.*, 2007; Roland *et al.*, 2007). As shown previously in other cell types, epitope-tagged EHD1, EHD3, and EHD4 were sometimes present on membrane tubules when expressed in SK-BR-3 cells (Figure 7, A–C). Myc-EHD3 was present on tubules more frequently than myc-EHD1, as reported previously in other cells (Galperin *et al.*, 2002). To determine the relationship between EHD tubules and caveolin-1 tubules, we coexpressed each protein in turn with caveolin-1-GFP in SK-BR-3 cells. All three proteins colocalized with caveolin-1-GFP in punctate structures and also in long tubules (Figure 7, D–F).

Because Rab8 can also localize to tubules that contain EHD proteins (Hattula *et al.*, 2006; Roland *et al.*, 2007), we coexpressed Rab8-GFP and caveolin-1-RFP in SK-BR-3 cells. Both wild-type GFP-Rab8 and constitutively active GFP-Rab8-Q67L colocalized with caveolin-1-RFP on tubules (Figure 7, H and I). Furthermore, caveolin-1-RFP and GFP-Rab8-Q67L synergized to promote tubule formation. When expressed individually, GFP-Rab8-Q67L and caveolin-1-RFP were present on long tubules in 16.2 and 13.7% of transfected cells, respectively (Figures 4G and 7G). Doubling the amount of each individual plasmid did not significantly increase the fraction of cells containing tubules (data not shown). By contrast, the two proteins were present together on tubules in 34.3% of cotransfected SK-BR-3 cells (Figure 7G). (We never saw cells that expressed both proteins in which one but not the other was localized to tubules.) This suggested that the two proteins contributed to tubule for-

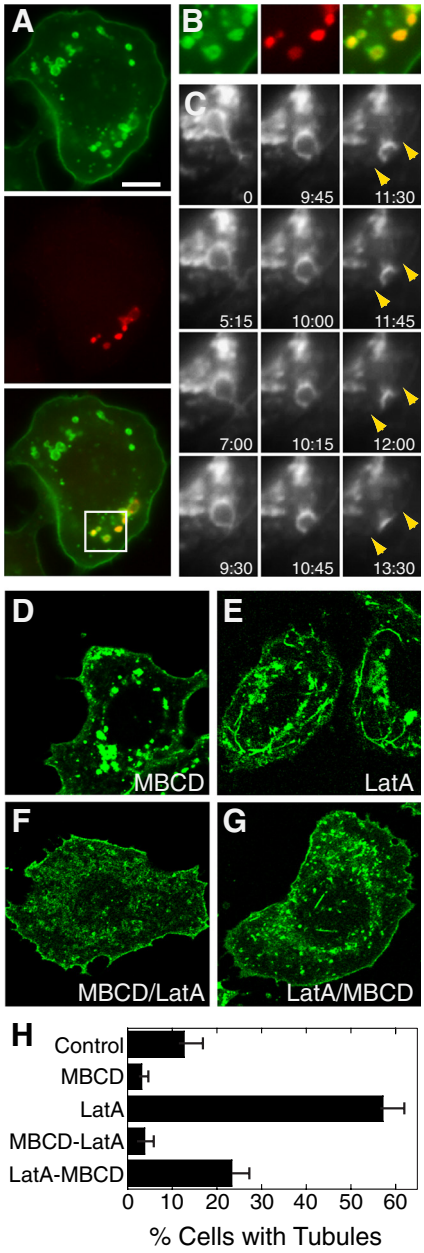

Figure 5. MBCD alters caveolin-1-GFP localization and reduces tubule frequency in SK-BR-3 cells. (A) SK-BR-3 cells expressing caveolin-1 GFP (top) were incubated with 10 mM MBCD for 45 min and then with 1 mM fluoro-ruby red dextran (middle) for 5 min before fixation and detection by fluorescence microscopy. (B) Enlarged views of the boxed region of the merged image of the cell shown in A. (C) Frames from Supplemental Movie 2, showing a live MBCD-treated SK-BR-3 cell expressing caveolin-1-GFP. A caveolin-1-GFP–positive vacuole that initially seems tethered to the plasma membrane approaches the plasma membrane (indicated with arrows in the last four frames) and fuses with it. Time elapsed (minutes:seconds) after the first frame is shown. (D–G) Images of caveolin-1-GFP–expressing SK-BR-3 cells treated with MBCD (30 min; D), LatA (10 min; E), MBCD (30 min) and then MBCD + LatA (10 min; F), or LatA (10 min) and then MBCD + LatA (30 min; G). Bar, 10 μm. (H) Frequency of caveolin-1 long tubules in cells treated as in D–G. The mean ± SEM of at least three experiments (counting at least 150 cells on each slide) is shown.

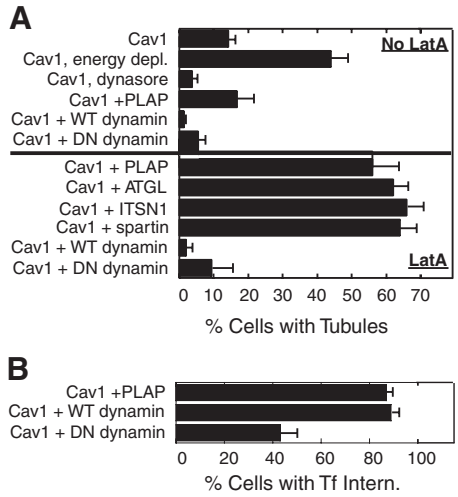

Figure 6. Caveolin-1 tubule frequency is enhanced by energy depletion and inhibited by both overexpression and inhibition of dynamin-2. Caveolin-1-GFP (Cav1; 1 μg of plasmid) was expressed in SK-BR-3 cells alone, or together with 3 μg of one of the following plasmids, as indicated: PLAP, HA-dynamin-2 (WT dynamin), HA-dynamin-2-K44A (DN dynamin), HA-ATGL, HA-ITSN1, or HA-spartin. (A) Where indicated, cells were energy-depleted or treated with dynasore as described under *Materials and Methods* or treated with LatA for 10 min (bottom half of graph). Cells were processed for immunofluorescence microscopy, detecting PLAP with anti-PLAP antibodies and the HA-tagged proteins with anti-HA antibodies. The percentage of cells expressing both caveolin-1-GFP and any cotransfected construct in which caveolin-1-GFP was in long tubules is shown. (B) Cells transfected with the indicated constructs were incubated with 35 μg/ml Texas Red-Tf for 5 min before fixation, and the percentage of caveolin-1-GFP–expressing cells containing internalized Tf (≥3 internal puncta) is shown. Expression of PLAP or the dynamin proteins in parallel dishes not incubated with Tf was verified by immunofluorescence microscopy; ≥85% of cells expressing caveolin-1-GFP also expressed the cotransfected construct. The mean ± SEM of at least three experiments (counting at least 150 cells on each slide) is shown.

mation through different mechanisms. Dominant-negative GFP-Rab8-T22N almost abolished caveolin-1-RFP tubules, both with and without LatA (Figure 7, G and J). Nevertheless, siRNA-mediated suppression of Rab8a by ~50% did not affect caveolin-1-GFP tubule formation (Supplemental Figure 4). We conclude that Rab8a affects, and may be essential for, tubule formation by caveolin-1-GFP. This effect may require only a low amount of Rab8a function, or another Rab may be able to substitute for Rab8 in this process, explaining the lack of effect of Rab8 knockdown.

The small GTPase Arf6 regulates formation of tubules containing EHD proteins (Caplan *et al*., 2002) and also those containing Rab8 (Hattula *et al*., 2006). In both cases, constitutively active Arf6-Q67L abolishes tubules. Similarly, caveolin-1-GFP–positive long tubules were greatly reduced in cells expressing Arf6-Q67L (Figure 7G). Arf6-Q67L interrupts endocytosis and recycling, and enlarged early endocytic vacuoles accumulate in cells expressing this protein (Naslavsky *et al*., 2004). Caveolin-1-GFP was present together with Arf6-Q67L on vacuoles in SK-BR-3 cells, suggesting that it traffics via an Arf6-regulated pathway (Figure 7K). GPI-anchored proteins are also internalized by an Arf6-regulated pathway (Naslavsky *et al*., 2004). As expected, the GPI-anchored protein PLAP colocalized with caveolin-1-GFP on tubules (Figure 7L).

Thus, caveolin-1 long tubules are closely related to Rab8/EHD protein tubules described previously (Hattula *et al*.,

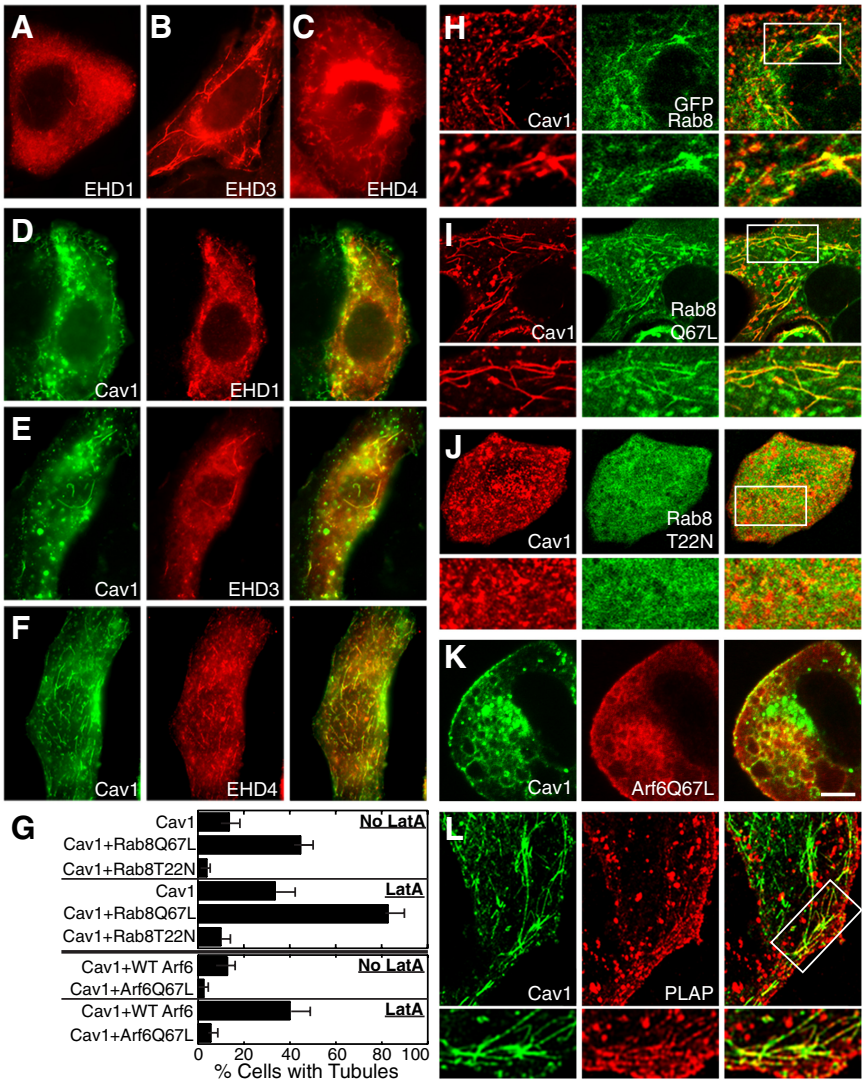

Figure 7. Rab8 and EHD proteins colocalize with caveolin-1 on tubules, whereas Arf6 antagonizes tubule formation. (A–C) SK-BR-3 cells expressing myc-EHD1, myc-EHD3, or HA-EHD4 as indicated were visualized by immunofluorescence microscopy by using anti-myc or anti-HA antibodies. All three proteins were seen on membrane tubules. (D–F) Caveolin-1-GFP (left) was coexpressed with myc-EHD1 (D), myc-EHD3 (E), or HA-EHD4 (F). Caveolin-1-GFP colocalized with all three proteins on puncta and tubules. (G) Top half, percentage of SK-BR-3 cells containing caveolin-1-RFP (Cav1)-positive tubules, after cotransfection with the indicated Rab8 constructs, with or without LatA. Rab8Q67L was always present on tubules in cells that also contained tubular caveolin-1-RFP. Bottom half, percent of SK-BR-3 cells containing caveolin-1-GFP (Cav1)-positive tubules after transfection with the indicated HA-tagged Arf6 constructs, with or without LatA. The mean ± SEM of at least three experiments (counting at least 150 cells on each slide) is shown. (H-L) SK-BR-3 cells coexpressing caveolin-1-RFP (H–J) or caveolin-1-GFP (K and L) and either GFP-Rab8 (H), GFP-Rab8-Q67L (I), GFP-Rab8-T22N (J), Arf6-Q67L (K), or PLAP (L) were examined by fluorescence microscopy, detecting HA-Arf6-Q67L with anti-HA and PLAP with anti-PLAP antibodies. High-magnification views of the boxed region in the merged images (H–J and L, right) are shown beneath appropriate panels. Bar, 5 μm.

2006; Roland *et al.*, 2007) and are regulated by many of the same mechanisms. Both are microtubule-dependent, greatly enhanced by LatA, abolished by Arf6-Q67L, and labeled by Rab8 and EHD proteins. Our finding that Rab8Q67L and caveolin-1 synergize to promote tubule accumulation suggests that the two proteins act by different and complementary mechanisms.

To determine whether endogenous caveolin-1 were recruited to GFP-Rab8-Q67L- or myc-EHD3-induced tubules, we expressed these proteins separately in HeLa or MDA-MB-231 cells and examined them together with endogenous caveolin-1. Results were similar in the two cell lines: HeLa cell results are shown in Supplemental Figure 5. Both myc-EHD3 and GFP-Rab8-Q67L formed abundant tubules in these cells. Endogenous caveolin-1 was not present on these tubules, and neither myc-EHD3 nor GFP-Rab8-Q67L noticeably affected the cellular localization of caveolin-1. Caveolin-1 sometimes colocalized with myc-EHD3 and GFP-Rab8-Q67L in punctate structures, and caveolin-1–positive puncta were sometimes close to or at the ends of the tubules (arrows in Supplemental Figure 5). This might reflect a relationship between these structures, or simply association of both with the same microtubules.

Caveolin-1-GFP Short Tubules Depend on the Actin Cytoskeleton but Not on Microtubules

In addition to the long tubules described above, caveolin-1-GFP expressed in SK-BR-3 cells was also seen on short tubules. These were 2–3 μm long, tortuous and highly branched, and were restricted to the zone just under the plasma membrane that also contained the subcortical actin cytoskeleton (Figure 8A). Short tubules were often closely apposed to cortical actin filaments (Figure 8B). Small punctate caveolin-1-positive structures were also abundant in this region (Figures 2E and 8B). Like long tubules, short tubules were derived from the plasma membrane, because they could be labeled by CTxB in 2 min (Figure 8C) and by GFP-PH-PLCδ (Figure 8D) but not by Tf (Figure 8E). Also, like long tubules, short tubules were cholesterol dependent and were not seen in MBCD-treated cells (Figure 5A). Unlike long tubules, however, short tubules did not require microtubules, and in fact they seemed more abundant and extensive in nocodazole-treated cells. By contrast, short tubules required actin filaments and were never seen in LatA-treated cells. Live-cell imaging studies, described next, provided further insight into dynamics and cytoskeletal interactions of long and short tubules.

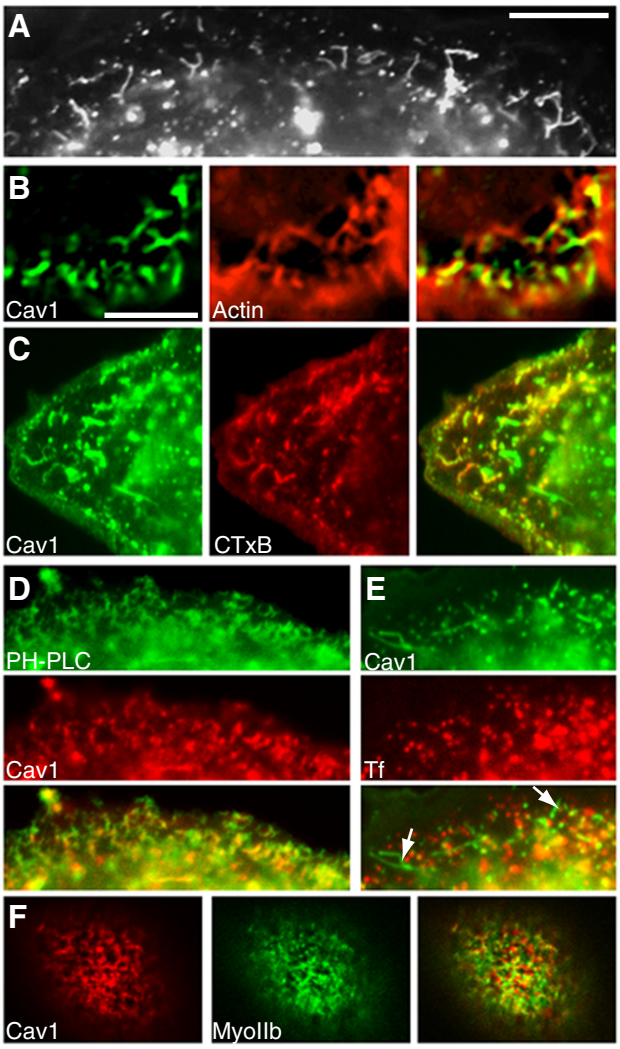

Figure 8. Short caveolin-1 tubules in SK-BR-3 cells are linked to actin and derived from the plasma membrane. (A) Section of a caveolin-1-GFP–expressing cell shows short, branched tubules just under the cell surface. (B) Cells expressing caveolin-1-GFP (left) were fixed, permeabilized, and treated with AF-594-phalloidin (middle). A cell section just under the plasma membrane (at the bottom and right of the image), containing short tubules close to actin filaments, is shown. (C) Cells expressing caveolin-1-GFP (left) were incubated with AF-594 CTxB (middle) for 2 min before fixation. Internalized CTxB-labeled puncta and short tubules near the cell periphery. (D) Cells coexpressing GFP-PH-PLCδ (top) and caveolin-1-RFP (middle) were processed for fluorescence microscopy. Caveolin-1-RFP–positive short tubules and puncta are labeled with GFP-PH-PLCδ. (E) Cells expressing caveolin-1-GFP (top) were incubated with AF-594 transferrin (middle) for 5 min. Caveolin-1-GFP–positive short tubules (arrows in merged image; bottom) are not labeled with transferrin. (F) Cells coexpressing caveolin-1-RFP (left) and GFP-myosin IIa (middle) were fixed and examined by fluorescence microscopy. High-magnification views of the boxed region in the merged image (right) are shown beneath each panel. Additional images of the same cell, showing dorsal stress fibers below the zone containing short tubules, are shown in Supplemental Figure 6. Bar in A, 10 μm. Bar in B (applies to B–F), 5 μm.

Actomyosin Interactions Exert Tension on Caveolin-1 Tubules

Both long and short tubules were often dynamic, with ends that extended and retracted during observation (Supplemental Movie 3, showing long tubules in a LatA-treated cell, although similar behavior was seen in control cells). In some of these cells, tubules seemed to be pulled from peripheral vacuoles (Supplemental Movie 3; selected frames shown in Figure 9A), although vacuoles near the cell center were less dynamic. Both long and short tubules seemed to be under tension. Segments of long tubules between branch points were generally straight, as if stretched taut (as seen in Figure 1A). Both long and short tubules were unstable, and they broke down fairly quickly. This occurred when tubules snapped, after which ends retracted. The resulting tubule fragments often resolved into motile puncta. Short fragments occasionally broke off and moved away from the parent tubule (data not shown). Short tubule dynamics are shown in Supplemental Movie 4 and Figure 9B and long tubules in Supplemental Movie 5 and Figure 9C. Short tubules behaved identically in control and nocodazole-treated cells. To facilitate viewing, the extensive short tubule network in a nocodazole-treated cell is shown. In Figure 9, B and C, arrows indicate positions where a tubule will have snapped in the next frame shown.

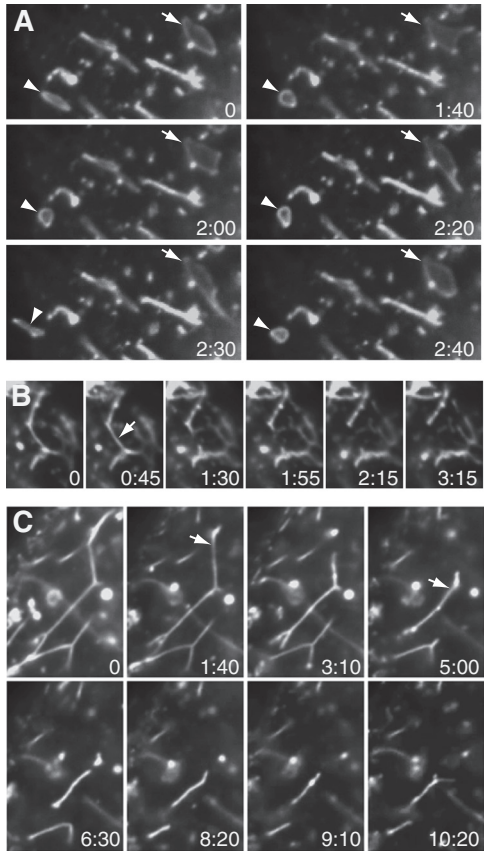

Figure 9. Dynamics of caveolin-1-GFP–positive tubules and vacuoles in SK-BR-3 cells expressing caveolin-1-GFP and examined by live-cell microscopy. (A) Frames from Supplemental Movie 3 of a LatA-treated cell. Arrow (top right) and arrowhead (bottom left) indicate two vacuoles that are transiently deformed. (B) Frames from Supplemental Movie 4, of a nocodazole-treated cell, showing short tubules. Arrow (second frame) indicates position where the tubule will have snapped by the next frame. (C) Frames from Supplemental Movie 5, showing long tubules. Arrows (second and fourth frames) indicate positions where tubules will have snapped by the next frame. (A–C) Time elapsed (minutes:seconds) after the first frame is shown. Images were captured every 10 s (A and C) or 15 s (B).

Table 1. Actin filaments and myosin II function are required for caveolin-1 tubule instability[a]

Construct expressed	Treatment	% decrease in long tubule length, 10 min
Cav-1-GFP	Control	68.5 ± 14.6, n = 8
Cav-1-GFP	LatA	15.4 ± 10.1, n = 5
Cav-1-RFP	Control	67.2 ± 14.2, n = 5
Cav-1-RFP	Blebbistatin	10.0 ± 4.8, n = 5

[a] Caveolin-1-GFP or caveolin-1-RFP as indicated was expressed in SK-BR-3 cells grown on glass-bottomed dishes for live-cell imaging. Cells were left untreated (control) or treated with LatA or blebbistatin for 30 min as indicated. Movies were made of cells chosen for the presence of abundant tubules. The total length of long tubules in one focal plane of one cell in a frame near the start of the movie, and a frame of the same movie taken 10 min later were measured, and the percentage of decrease in tubule length was calculated. Average percentage of decrease in tubule length in the indicated number of cells, ± SD, is shown.

Total tubule length in cells chosen on the basis of abundant tubules decreased substantially over the time of observation. Although this was true of both long and short tubules, it was easier to quantitate for long tubules. To do this, we measured total tubule length (in 1 focal plane) per cell in a frame captured at the start of observation, and another frame of the same cell taken 10 min later. Total tubule length at the start varied widely between cells (30–200 μm) but decreased by a fairly uniform amount (~70%) over 10 min (Table 1).

Long tubules were abundant and often remained highly dynamic after LatA treatment. Nevertheless, LatA affected tubule morphology and behavior. Long tubules in LatA-treated cells sometimes had a curved, slack appearance, suggesting they were under less tension than tubules in control cells (Figure 2D). A section of the control cell shown in Figure 1A is shown for comparison (Figure 2C). This relaxed tubule morphology was not seen in control cells. Furthermore, live-cell imaging showed that long tubules in LatA-treated cells rarely snapped and did not decline in abundance over the time of observation (Supplemental Movie 6 and Table 1). Together, these results suggested that long tubules interacted with actin filaments as well as microtubules and that interactions with the actin cytoskeleton induced strain on the tubules and enhanced their breakdown. Consistent with the possibility of such an interaction, long tubules often extended into the actin-rich zone just beneath the plasma membrane (Figure 2E).

Myosin II is responsible for cortical tension in the actomyosin cytoskeleton (Paluch *et al*., 2006; Clark *et al*., 2007). Myosin II is present in stress fibers. In addition to the familiar ventral stress fibers near the bottom of the cell, myosin II is also present in dorsal stress fibers and transverse arcs close to the top of the cell (Pellegrin and Mellor, 2007). GFP-myosin IIa and GFP-myosin IIb had similar localization patterns when expressed in SK-BR-3 cells. Both were present in stress fibers near both dorsal and ventral surfaces of transfected SK-BR-3 cells. (Because we could not distinguish dorsal stress fibers and transverse arcs, we refer to all stress fibers near the dorsal cell surface as dorsal.) Neither short nor long caveolin-1 tubules were closely associated with stress fibers in either location. However, GFP-myosin IIa-positive puncta and short filaments were also seen in a zone above the layer of dorsal stress fibers, just under the dorsal cell surface. Caveolin-1 short tubules were localized to this zone and were often closely associated with GFP-myosin IIa in this region (Figure 8F and Supplemental Figure 6).

To determine whether myosin II exerted tension on caveolin-1 long tubules, we examined tubule stability in cells treated with the myosin II inhibitor blebbistatin. As blebbistatin induces phototoxicity in live cells expressing GFP-tagged proteins (Kolega, 2004), we expressed caveolin-1-RFP in these experiments. Rapid bleaching of RFP made tubule dynamics harder to visualize than in cells expressing caveolin-1-GFP. Nevertheless, caveolin-1-RFP tubules showed similar behavior to caveolin-1-GFP tubules. Tubules snapped, and tubule length decreased over time (Supplemental Movie 7 and Table 1). By contrast, tubule snapping was less frequent in blebbistatin-treated cells, and tubules remained more stable (Supplemental Movie 8 and Table 1). We conclude that myosin II induces tension on caveolin-1–positive membrane tubules, leading to snapping and destabilization.

DISCUSSION

Caveolin-1 Tubule Formation and Dynamics

Although tubules were seen in only a small fraction of cells, they were often abundant in these cells. This suggests that a triggering event (possibly a stochastic spike in signaling activity) in an individual cell occasionally leads to rapid and sometimes abundant tubule formation. The fact that we did not observe tubules forming de novo suggests that this event is rare. Our results suggest that microtubule-dependent motors at the tips of long tubules pull membrane tubules inward from the plasma membrane as the motors move along microtubules. Short tubules do not interact with microtubule-dependent motors but may be formed by an analogous process involving cortical actin filaments and myosin II. Long tubules also bind actomyosin: this interaction exerts tension on both long and short tubules, causing them to break. LatA increases long tubule abundance at least in part by stabilizing the tubules: we do not know whether LatA also increases the rate of tubule formation.

Caveolins have been proposed to deform the plasma membrane to form caveolae (Shnyrova *et al*., 2008). Our results suggest that caveolin-1 may deform the plasma membrane to form tubules in cancer cells by the same mechanism. Our results suggest that PTRF/cavin-1 is an important inhibitor of caveolin-1 tubule formation. We showed for the first time that PTRF/cavin-1 and caveolin-1 are lost coordinately in cancer cells. The lack of PTRF/cavin-1 in these cells explained the ability of caveolin-1 to form tubules upon reexpression. The fact that depletion of PTRF/cavin-1 in MDA-MB-231 cells permitted tubule formation by endogenous caveolin-1 suggests that this mechanism is important in normal cells as well. These findings define an important new role for PTRF/cavin-1 in regulating caveolin-1 membrane dynamics.

In contrast to this activity of PTRF/cavin-1, the closely related protein SDPR/cavin-2 enlarges caveolae when expressed at moderate levels, and stimulates tubule formation at high levels (Hansen *et al*., 2009). PTRF/cavin-1 and SDPR/cavin-2 can bind each other and are both present in caveolae. It is possible that interaction between these proteins, one promoting and one inhibiting membrane deformation, may help fine-tune the extent of caveolae formation.

Caveolin-1 tubule accumulation in normal cells might also be reduced by dynamin-mediated scission, as we found that overexpressing dynamin-2 reduced tubule formation. It remains unclear why dynamin-2 should act less efficiently in

caveolar scission in cancer cells than normal cells, when other dynamin-dependent process (such as clathrin-mediated endocytosis) seem normal. Furthermore, we do not know why inhibiting dynamin function also abolished caveolin-1 tubules. Dynamins are multifunctional and participate in functions independent of scission, often together with actin (Kruchten and McNiven, 2006). Different dynamin-dependent effects may affect caveolin-1 tubules in different ways.

How Caveolin-1 Tubules Associate with Cytoskeleton

Caveolae are closely associated with actin filaments and microtubules (Richter *et al*., 2008). Caveolin-1-GFP–positive vesicles move in a bidirectional, microtubule-dependent manner, showing that they bind microtubules (Mundy *et al*., 2002). Lateral mobility of caveolae in the plasma membrane increases dramatically upon disruption of actin filaments, suggesting that caveolae are directly linked to actin filaments (Mundy *et al*., 2002; Pelkmans *et al*., 2002; Thomsen *et al*., 2002). However, the low mobility of caveolae might also be explained by steric trapping of caveolae in the cortical actin meshwork (Tagawa *et al*., 2005).

We found that caveolin-1 long tubules were linked both to microtubules and actin filaments, whereas short tubules bound actin filaments. Tubules in SK-BR-3 cells probably interact with cytoskeletal elements in the same manner as caveolae in normal cells. If so, then this interaction would induce tension on caveolae, although their morphology would make this hard to detect. As detailed next, this tension might aid in caveolar scission from the membrane, as has been suggested to occur in scission of clathrin-coated vesicles. In addition, in a role that may be unique to caveolae, constitutive tension on caveolar membranes might contribute to their function, explaining how caveolin-1 regulates processes that depend on the actin cytoskeleton. At least two such functions have been described: mechanosensation (Parton and Simons, 2007) and directional cell migration (Sun *et al*., 2007; Grande-García and del Pozo, 2008). Actomyosin-induced stretching might alter the conformation of caveolin-1 or another caveolar protein that sensed tension, as occurs for some actin-binding proteins (Vogel and Sheetz, 2009). Alternatively, mechanical force might affect the membrane elasticity of the raft-like caveolar membrane, thereby affecting the function of caveolar proteins by changing the physical properties of the surrounding bilayer, as suggested previously (Parton and Simons, 2007). By such mechanisms, local changes in actomyosin-induced tension on the caveolar membrane could differentially affect the function of caveolar proteins in different regions of the cell surface.

Role of Tension in Caveolin-1 Tubule Scission

Several groups have studied microtubule-dependent tubule formation in vitro. In early studies, tubules formed when motors were added to ER- or Golgi-derived vesicles in contact with microtubules immobilized on a solid support (Dabora and Sheetz, 1988; Allan and Vale, 1994). Later work showed that motors bound to artificial liposomes placed on immobilized microtubules could pull tubules from the liposomes (Roux *et al*., 2002; Koster *et al*., 2003; Shaklee *et al*., 2008). These tubules resembled the long caveolin-1–dependent tubules we observed, suggesting that they formed by a similar mechanism. As we saw for caveolin-1–positive long tubules, microtubule-dependent tubules formed in vitro do not always precisely colocalize with microtubules (Allan and Vale, 1994). In the in vitro studies, this probably resulted from the fact that motors were concentrated at the tips of tubules (Allan and Vale, 1994; Shaklee *et al*., 2008). Shaklee *et al*. (2008) proposed that lipid-bound microtubule motors can concentrate at tubule tips because motor off-rate is inversely proportional to force and noted that lipid-bound motors on a tubule cannot exert force unless they are at a tubule tip (Shaklee *et al*., 2008). Further work is required to determine whether microtubule motors on caveolin-1–positive membranes show similar characteristics.

Although tubule ends might extend and retract (Koster *et al*., 2003), tubule breakage in microtubule-dependent in vitro systems has not been widely reported. Similarly, we observed little tubule breakage in LatA-treated cells, although long tubules presumably interacted with microtubule-dependent motors and microtubules. This suggested that microtubule-dependent motors do not exert enough force to break the tubules; they would probably stall before that could occur. By contrast, in untreated SK-BR-3 cells, both long and short caveolin-1 tubules often broke, after which ends retracted. The different behavior of long tubules in control and LatA- or blebbistatin-treated cells showed that actomyosin interactions were required for tubule breakage, probably by increasing tension on the tubules. The same was probably true of short tubules, which were closely associated with actin and myosin II filaments, although we could not show this directly as short tubules required actin filaments to form. This tension might have been sufficient to break tubules. Alternatively, tubule scission might have been mediated by proteins. Dynamins can break tubules in vitro, but only if the tubules are under tension (Roux *et al*., 2006). This property has been proposed to help explain how actin and dynamin cooperate in scission of clathrin-coated vesicles from the plasma membrane (Roux *et al*., 2006). New actin polymerization at the site of clathrin-coated pit formation may stretch the nascent pit, pushing it away from the membrane (Kaksonen *et al*., 2005; Merrifield *et al*., 2005). The resulting tension in the neck of the pit has been suggested to facilitate scission by dynamins (Roux *et al*., 2006). Caveolar endocytosis also depends on dynamins (Oh *et al*., 1998; Pelkmans *et al*., 2002), and tension might be induced in the same manner as in clathrin-coated pits. However, as caveolae are probably linked to actin filaments even when they are not undergoing endocytosis (Richter *et al*., 2008), they may experience constitutive tension. Dynamins might use this tension, rather than tension induced by a protrusive effect of new actin polymerization pushing against a membrane just before scission occurs, in caveolar endocytosis. Dynamins, or possibly EHD proteins, might cleave caveolin-1–positive tubules in SK-BR-3 cells in a tension-dependent manner. The increased frequency of long tubules we observed in LatA-treated cells might reflect increased tubule stability under conditions where breakage was inhibited. Further work will show whether actomyosin-induced tension on caveolae underlies the function of caveolin-1 in actin-related functions such as mechanosensation and directional cell migration.

Relationship of Caveolin-1 Tubules to EHD Proteins and Rab8

Both EHD proteins and Rab8 colocalized with caveolin-1 on tubules. Tubular localization of both EHD proteins and Rab8 has been reported previously (Caplan *et al*., 2002; Galperin *et al*., 2002; Hattula *et al*., 2006; Roland *et al*., 2007; Jovic *et al*., 2009), and EHD proteins and Rab8 were present on the same tubules when coexpressed in HeLa cells (Roland *et al*., 2007; Jovic *et al*., 2009). Like caveolin-1 long tubules, these tubules are microtubule dependent and regulated by Arf6. In addition, actin depolymerization increases the frequency of both caveolin-1 tubules and Rab8 tubules. Together with the fact that caveolin-1 colocalized with both EHD proteins and

Rab8 on tubules, these observations suggested that tubules containing the three proteins were formed and regulated by similar mechanisms.

EHD proteins have structural and mechanistic features in common with dynamins, although they hydrolyze ATP instead of guanosine triphosphate (Daumke *et al*., 2007). Like dynamins, purified EHD2 can tubulate model membranes, oligomerizing to form ring-like structures around the tubules (Daumke *et al*., 2007). An EHD2 mutant defective for ATP hydrolysis was associated with tubules more frequently, and with small vesicles less frequently, than the wild-type protein when expressed in HeLa cells (Daumke *et al*., 2007). This suggested that EHD proteins, like dynamins, might mediate vesicle scission in a manner that depends on nucleotide hydrolysis. Membrane-stimulated nucleotide hydrolysis by EHD2 is 600-fold slower than by dynamin (Daumke *et al*., 2007), possibly explaining why overexpressed wild-type EHD proteins sometimes localize to tubules, whereas dynamin does not.

Rab8 probably localizes to tubules and induces tubule formation indirectly, through tubule-promoting effector proteins. It is possible that these include EHD proteins. Our finding that caveolin-1-GFP colocalized with both Rab8 and EHD proteins on tubules raised the possibility that the proteins function together, possibly in recycling (Naslavsky and Caplan, 2005; Jovic *et al*., 2009). Alternatively, EHD proteins might be recruited to caveolin-1 tubules because of their structure. Structural characterization suggested that EHD2 has a highly curved membrane interaction domain (Daumke *et al*., 2007). This structure would allow the protein to tubulate membranes and should also favor its recruitment to preexisting highly curved membrane tubules. EHD proteins bind phosphoinositides, sometimes with unusually low specificity (Blume *et al*., 2007; Naslavsky *et al*., 2007; Daumke *et al*., 2007). The presence of $PI(4,5)P_2$ or another phosphoinositide on caveolin-1-GFP tubules, together with their high curvature, may be sufficient to recruit EHD proteins.

ACKNOWLEDGMENTS

We thank the following for plasmids: Tamás Balla, Craig Blackstone, Catherine Jackson, Steven Caplan, James Casanova, Simon Halegoua, Ari Helenius, Allan Levey, Douglas Lublin, William Maltese, John O'Bryan, Johan Peränen, Michelle Peckham, Paul Pilch, Enrique Rodriguez-Boulan, and Sandra Schmid. This work was supported by National Institutes of Health grant GM-47897 (to D.A.B).

REFERENCES

Albinsson, S., Nordstrom, I., Sward, K., and Hellstrand, P. (2008). Differential dependence of stretch and shear stress signaling on caveolin-1 in the vascular wall. Am. J. Physiol. Cell Physiol. *294*, C271–C279.

Allan, V., and Vale, R. (1994). Movement of membrane tubules along microtubules in vitro: evidence for specialised sites of motor attachment. J. Cell Sci. *107*, 1885–1897.

Ang, A. L., Fölsch, H., Koivisto, U. M., Pypaert, M., and Mellman, I. (2003). The Rab8 GTPase selectively regulates AP-1B–dependent basolateral transport in polarized Madin-Darby canine kidney cells. J. Cell Biol. *163*, 339–350.

Bakowska, J. C., Jupille, H., Fatheddin, P., Puertollano, R., and Blackstone, C. (2007). Troyer syndrome protein spartin is mono-ubiquitinated and functions in EGF receptor trafficking. Mol. Biol. Cell *18*, 1683–1692.

Barr, D. J., Ostermeyer-Fay, A. G., Matundan, R. A., and Brown, D. A. (2008). Clathrin-independent endocytosis of ErbB2 in geldanamycin-treated human breast cancer cells. J. Cell Sci. *121*, 3155–3166.

Bastiani, M., *et al*. (2009). MURC/Cavin-4 and cavin family members form tissue-specific caveolar complexes. J. Cell Biol. *185*, 1259–1273.

Berger, J., Howard, A. D., Gerber, L., Cullen, B. R., and Udenfriend, S. (1987). Expression of active, membrane-bound human placental alkaline phosphatase by transfected simian cells. Proc. Natl. Acad. Sci. USA *84*, 4885–4889.

Blume, J. J., Halbach, A., Behrendt, D., Paulsson, M., and Plomann, M. (2007). EHD proteins are associated with tubular and vesicular compartments and interact with specific phospholipids. Exp. Cell Res. *313*, 219–231.

Boyd, N. L., Park, H., Yi, H., Boo, Y. C., Sorescu, G. P., Sykes, M., and Jo, H. (2003). Chronic shear induces caveolae formation and alters ERK and Akt responses in endothelial cells. Am. J. Physiol. Heart Circ. Physiol. *285*, H1113–H1122.

Caplan, S., Naslavsky, N., Hartnell, L. M., Lodge, R., Polishchuk, R. S., Donaldson, J. G., and Bonifacino, J. S. (2002). A tubular EHD1-containing compartment involved in the recycling of major histocompatibility complex class I molecules to the plasma membrane. EMBO J. *21*, 2557–2567.

Charafe-Jauffret, E., *et al*. (2007). Moesin expression is a marker of basal breast carcinomas. Int. J. Cancer *121*, 1779–1785.

Clark, K., Langeslag, M., Figdor, C. G., and van Leeuwen, F. N. (2007). Myosin II and mechanotransduction: a balancing act. Trends Cell Biol. *17*, 178–186.

Cremona, O., *et al*. (1999). Essential role of phosphoinositide metabolism in synaptic vesicle recycling. Cell *99*, 179–188.

Dabora, S. L., and Sheetz, M. P. (1988). The microtubule-dependent formation of a tubulovesicular network with characteristics of the ER from cultured cell extracts. Cell *54*, 27–35.

Daumke, O., Lundmark, R., Vallis, Y., Martens, S., Butler, P.J.G., and McMahon, H. T. (2007). Architectural and mechanistic insights into an EHD ATPase involved in membrane remodelling. Nature *449*, 923–927.

Denker, S. P., McCaffrey, J. M., Palade, G. E., Insel, P. A., and Farquhar, M. G. (1996). Differential distribution of alpha subunits and beta-gamma subunits of heterotrimeric G proteins on Golgi membranes of the exocrine pancreas. J. Cell Biol. *133*, 1027–1040.

Dunn, S., Morrison, E. E., Liverpool, T. B., Molina-Paris, C., Cross, R. A., Alonso, M. C., and Peckham, M. (2008). Differential trafficking of Kif5c on tyrosinated and detyrosinated microtubules in live cells. J. Cell Sci. *121*, 1085–1095.

Eastman, S. W., Yassaee, M., and Bieniasz, P. D. (2009). A role for ubiquitin ligases and Spartin/SPG20 in lipid droplet turnover. J. Cell Biol. *184*, 881–894.

Finn, R. S., Dering, J., Ginther, C., Wilson, C. A., Glaspy, P., Tchekmedyian, N., and Slamon, D. J. (2007). Dasatinib, an orally active small molecule inhibitor of both the src and abl kinases, selectively inhibits growth of basal-type/"triple-negative" breast cancer cell lines growing in vitro. Breast Cancer Res. Treat. *105*, 319–326.

Fiucci, G., Ravid, D., Reich, R., and Liscovitch, M. (2002). Caveolin-1 inhibits anchorage-independent growth, anoikis and invasiveness in MCF-7 human breast cancer cells. Oncogene *21*, 2365–2375.

Galperin, E., Benjamin, S., Rapaport, D., Rotem-Yehudar, R., Tolchinsky, S., and Horowitz, M. (2002). EHD *3*, A protein that resides in recycling tubular and vesicular membrane structures and interacts with EHD1. Traffic *3*, 575–589.

George, M., Ying, G., Rainey, M. A., Solomon, A., Parikh, P. T., Gao, Q., Band, V., and Band, H. (2007). Shared as well as distinct roles of EHD proteins revealed by biochemical and functional comparisons in mammalian cells and *C. elegans*. BMC Cell Biol. *8*, 3

Gillooly, D. J., Morrow, I. C., Lindsay, M., Gould, R., Bryant, N. J., Gaullier, J. M., Parton, R. G., and Stenmark, H. (2000). Localization of phosphatidylinositol 3-phosphate in yeast and mammalian cells. EMBO J. *19*, 4577–4588.

Goetz, J. G., Lajoie, P., Wiseman, S. M., and Nabi, I. R. (2008). Caveolin-1 in tumor progression: the good, the bad and the ugly. Cancer Metastasis Rev. *27*, 715–735.

Grande-García, A., and del Pozo, M. A. (2008). Caveolin-1 in cell polarization and directional migration. Eur. J. Cell Biol. *87*, 641–647.

Grande-García, A., Echarri, A., de Rooij, J., Alderson, N. B., Waterman-Storer, C. M., Valdivielso, J. M., and del Pozo, M. A. (2007). Caveolin-1 regulates cell polarization and directional migration through Src kinase and Rho GTPases. J. Cell Biol. *177*, 683–694.

Hailstones, D., Sleer, L. S., Parton, R. G., and Stanley, K. K. (1998). Regulation of caveolin and caveolae by cholesterol in MDCK cells. J. Lipid. Res. *39*, 369–379.

Hansen, C. G., Bright, N. A., Howard, G., and Nichols, B. J. (2009). SDPR induces membrane curvature and functions in the formation of caveolae. Nat. Cell Biol. *11*, 807–814.

Hattula, K., Furuhjelm, J., Tikkanen, J., Tanhuanpää, K., Laakkonen, P., and Peränen, J. (2006). Characterization of the Rab8-specific membrane traffic route linked to protrusion formation. J. Cell Sci. *119*, 4866–4877.

Hernández-Deviez, D. J., Roth, M. G., Casanova, J. E., and Wilson, J. M. (2004). ARNO and ARF6 regulate axonal elongation and branching through down-

stream activation of phosphatidylinositol 4-phosphate 5-kinase alpha. Mol. Biol. Cell *15*, 111–120.

Hill, M. M., *et al*. (2008). PTRF-Cavin, a conserved cytoplasmic protein required for caveola formation and function. Cell *132*, 113–124.

Hommelgaard, A. M., Lerdrup, M., and van Deurs, B. (2004). Association with membrane protrusions makes ErbB2 an internalization-resistant receptor. Mol. Biol. Cell *15*, 1557–1567.

Huber, L. A., Pimplikar, S., Parton, R. G., Vira, H., Zerial, M., and Simons, K. (1993). Rab8, a small GTPase involved in vesicular traffic between the TGN and the basolateral membrane. J. Cell Biol. *123*, 35–45.

Jovic, M., Kieken, F., Naslavsky, N., Sorgen, P. L., and Caplan, S. (2009). EHD1-associated tubules contain phosphatidylinositol-4-phosphate and phosphatidylinositol-(4,5)-bisphosphate and are required for efficient recycling. Mol. Biol. Cell *20*, 2731–2743.

Kaksonen, M., Toret, C. P., and Drubin, D. G. (2005). A modular design for the clathrin- and actin-mediated endocytosis machinery. Cell *123*, 305–320.

Kalia, M., Kumari, S., Chadda, R., Hill, M. M., Parton, R. G., and Mayor, S. (2006). Arf6-independent GPI-anchored protein-enriched early endosomal compartments fuse with sorting endosomes via a Rab5/phosphatidylinositol-3′-kinase–dependent machinery. Mol. Biol. Cell *17*, 3689–3704.

Kilsdonk, E.P.C., Yancey, P. G., Stoudt, G. W., Bangerter, F. W., Johnson, W. J., Phillips, M. C., and Rothblat, G. H. (1995). Cellular cholesterol efflux mediated by cyclodextrins. J. Biol. Chem. *270*, 17250–17256.

Kolega, J. (2004). Phototoxicity and photoinactivation of blebbistatin in UV and visible light. Biochem. Biophys. Res. Commun. *320*, 1020–1025.

Koster, G., VanDuijn, M., Hofs, B., and Dogterom, M. (2003). Membrane tube formation from giant vesicles by dynamic association of motor proteins. Proc. Natl. Acad. Sci. USA *100*, 15583–15588.

Kruchten, A. E., and McNiven, M. A. (2006). Dynamin as a mover and pincher during cell migration and invasion. J. Cell Sci. *119*, 1683–1690.

Lacroix, M. (2009). MDA-MB-435 cells are from melanoma, not from breast cancer. Cancer Chemother. Pharmacol. *63*, 567.

Le Lay, S., and Kurzchalia, T. V. (2005). Getting rid of caveolins: phenotypes of caveolin-deficient animals. Biochim. Biophys. Acta *1746*, 322–333.

Linder, M. D., Uronen, R.-L., Hölttä-Vuori, M., van der Sluijs, P., Peränen, J., and Ikonen, E. (2007). Rab8-dependent recycling promotes endosomal cholesterol removal in normal and sphingolipidosis cells. Mol. Biol. Cell *18*, 47–56.

Liu, L., Brown, D., McKee, M., LeBrasseur, N. K., Yang, D., Albrecht, K. H., Ravid, K., and Pilch, P. F. (2008). Deletion of cavin/PTRF causes global loss of caveolae, dyslipidemia, and glucose intolerance. Cell Metab. *8*, 310–317.

Liu, L., and Pilch, P. F. (2008). A critical role of cavin (polymerase I and transcript release factor) in caveolae formation and organization. J. Biol. Chem. *283*, 4314–4322.

Macia, E., Ehrlich, M., Massol, R., Boucrot, E., Brunner, C., and Kirchhausen, T. (2006). Dynasore, a cell-permeable inhibitor of dynamin. Dev. Cell *10*, 839–850.

McMahon, K. A., Zajicek, H., Li, W. P., Peyton, M. J., Minna, J. D., Hernandez, V. J., Luby-Phelps, K., and Anderson, R. G. (2009). SRBC/cavin-3 is a caveolin adapter protein that regulates caveolae function. EMBO J. *28*, 1001–1015.

Merrifield, C. J., Perrais, D., and Zenisek, D. (2005). Coupling between clathrin-coated-pit invagination, cortactin recruitment, and membrane scission observed in live cells. Cell *121*, 593–606.

Milovanova, T., Chatterjee, S., Hawkins, B. J., Hong, N., Sorokina, E. M., Debolt, K., Moore, J. S., Madesh, M., and Fisher, A. B. (2008). Caveolae are an essential component of the pathway for endothelial cell signaling associated with abrupt reduction of shear stress. Biochim. Biophys. Acta *1783*, 1866–1875.

Mohney, R. P., Das, M., Bivona, T. G., Hanes, R., Adams, A. G., Philips, M. R., and O'Bryan, J. P. (2003). Intersectin activates Ras but stimulates transcription through an independent pathway involving JNK. J. Biol. Chem. *278*, 47038–47045.

Mora, R., Bonilha, V. L., Marmorstein, A., Scherer, P. E., Brown, D., Lisanti, M. P., and Rodriguez-Boulan, E. (1999). Caveolin-2 localizes to the Golgi complex but redistributes to plasma membrane, caveolae, and rafts when co-expressed with caveolin-1. J. Biol. Chem. *274*, 25708–25717.

Mundy, D. I., Machleidt, T., Ying, Y.-S., Anderson, R.G.W., and Bloom, G. S. (2002). Dual control of caveolar membrane traffic by microtubules and the actin cytoskeleton. J. Cell Sci. *115*, 4327–4339.

Naslavsky, N., and Caplan, S. (2005). C-terminal EH-domain-containing proteins: consensus for a role in endocytic trafficking, EH? J. Cell Sci. *118*, 4093–4101.

Naslavsky, N., Rahajeng, J., Chenavas, S., Sorgen, P. L., and Caplan, S. (2007). EHD1 and Eps15 interact with phosphatidylinositols via their Eps15 homology domains. J. Biol. Chem. *282*, 16612–16622.

Naslavsky, N., Weigert, R., and Donaldson, J. G. (2003). Convergence of non-clathrin- and clathrin-derived endosomes involves Arf6 inactivation and changes in phosphoinositides. Mol. Biol. Cell *14*, 417–431.

Naslavsky, N., Weigert, R., and Donaldson, J. G. (2004). Characterization of a nonclathrin endocytic pathway: membrane cargo and lipid requirements. Mol. Biol. Cell *15*, 3542–3552.

Oh, P., McIntosh, D. P., and Schnitzer, J. E. (1998). Dynamin at the neck of caveolae mediates their budding to form transport vesicles by GTP-driven fission from the plasma membrane of endothelium. J. Cell Biol. *141*, 101–114.

Ostermeyer, A. G., Paci, J. M., Zeng, Y., Lublin, D. M., Munro, S., and Brown, D. A. (2001). Accumulation of caveolin in the endoplasmic reticulum redirects the protein to lipid storage droplets. J. Cell Biol. *152*, 1071–1078.

Ostermeyer, A. G., Ramcharan, L. T., Zeng, Y., Lublin, D. M., and Brown, D. A. (2004). Role of the hydrophobic domain in targeting caveolin-1 to lipid droplets. J. Cell Biol. *164*, 69–78.

Paluch, E., Sykes, C., Prost, J., and Bornens, M. (2006). Dynamic modes of the cortical actomyosin gel during cell locomotion and division. Trends Cell Biol. *16*, 5–10.

Parton, R. G., Joggerst, B., and Simons, K. (1994). Regulated internalization of caveolae. J. Cell Biol. *127*, 1199–1216.

Parton, R. G., and Simons, K. (2007). The multiple faces of caveolae. Nat. Rev. Mol. Cell Biol. *8*, 185–194.

Pelkmans, L., Bürli, T., Zerial, M., and Helenius, A. (2004). Caveolin-stabilized membrane domains as multifunctional transport and sorting devices in endocytic membrane traffic. Cell *118*, 767–780.

Pelkmans, L., Kartenbeck, J., and Helenius, A. (2001). Caveolar endocytosis of simian virus 40 reveals a new two-step vesicular-transport pathway to the ER. Nat. Cell Biol. *3*, 473–483.

Pelkmans, L., Püntener, D., and Helenius, A. (2002). Local actin polymerization and dynamin recruitment in SV40-induced internalization of caveolae. Science *296*, 535–539.

Pellegrin, S., and Mellor, H. (2007). Actin stress fibers. J. Cell Sci. *120*, 3491–3499.

Peränen, J., Auvinen, P., Virta, H., Wepf, R., and Simons, K. (1996). Rab8 promotes polarized membrane transport through reorganization of actin and microtubules in fibroblasts. J. Cell Biol. *135*, 153–167.

Perrone, G., Altomare, V., Zagami, M., Morini, S., Petitti, T., Battista, C., Muda, A. O., and Rabitti, C. (2009). Caveolin-1 expression in human breast lobular cancer progression. Mod. Pathol. *22*, 71–78.

Peters, P. J., *et al*. (2003). Trafficking of prion proteins through a caveolae-mediated endosomal pathway. J. Cell Biol. *162*, 703–717.

Quest, A. F., Gutierrez-Pajares, J. L., and Torres, V. A. (2008). Caveolin-1, an ambiguous partner in cell signalling and cancer. J. Cell. Mol. Med. *12*, 1130–1150.

Ren, X., Ostermeyer, A. G., Ramcharan, L. T., Zeng, Y., Lublin, D. M., and Brown, D. A. (2004). Conformational defects slow Golgi exit, block oligomerization, and reduce raft affinity of caveolin-1 mutant proteins. Mol. Biol. Cell *15*, 4556–4567.

Richter, T., Floetenmeyer, M., Ferguson, C., Galea, J., Goh, J., Lindsay, M. R., Morgan, G. P., Marsh, B. J., and Parton, R. G. (2008). High-resolution 3D quantitative analysis of caveolar ultrastructure and caveola–cytoskeleton interactions. Traffic *9*, 893–909.

Rizzo, V., Morton, C., DePaola, N., Schnitzer, J. E., and Davies, P. F. (2003). Recruitment of endothelial caveolae into mechanotransduction pathways by flow conditioning in vitro. Am. J. Physiol. Heart Circ. Physiol. *285*, H1720–H1729.

Roland, J. T., Kenworthy, A. K., Peranen, J., Caplan, S., and Goldenring, J. R. (2007). Myosin Vb interacts with Rab8a on a tubular network containing EHD1 and EHD3. Mol. Biol. Cell *18*, 2828–2837.

Römer, W., *et al*. (2007). Shiga toxin induces tubular membrane invaginations for its uptake into cells. Nature *450*, 670–675.

Rothberg, K. G., Heuser, J. E., Donzell, W. C., Ying, Y.-S., Glenney, J. R., and Anderson, R.G.W. (1992). Caveolin, a protein component of caveolae membrane coats. Cell *68*, 673–682.

Roux, A., Cappello, G., Cartaud, J., Prost, J., Goud, B., and Bassereau, P. (2002). A minimal system allowing tubulation with molecular motors pulling on giant liposomes. Proc. Natl. Acad. Sci. USA *99*, 5394–5399.

Roux, A., Uyhazi, K., Frost, A., and De Camilli, P. (2006). GTP-dependent twisting of dynamin implicates constriction and tension in membrane fission. Nature *441*, 528–531.

Sahlender, D. A., Roberts, R. C., Arden, S. D., Spudich, G., Taylor, M. J., Luzio, J. P., Kendrick-Jones, J., and Buss, F. (2005). Optineurin links myosin VI to the Golgi complex and is involved in Golgi organization and exocytosis. J. Cell Biol. *169*, 285–295.

Sato, T., *et al*. (2007). The Rab8 GTPase regulates apical protein localization in intestinal cells. Nature *448*, 366–369.

Schroeder, R. J., Ahmed, S. N., Zhu, Y., London, E., and Brown, D. A. (1998). Cholesterol and sphingolipid enhance the Triton X-100-insolubility of GPI-anchored proteins by promoting the formation of detergent-insoluble ordered membrane domains. J. Biol. Chem. *273*, 1150–1157.

Schuck, S., Manninen, A., Honsho, M., Fullekrug, J., and Simons, K. (2004). Generation of single and double knockdowns in polarized epithelial cells by retrovirus-mediated RNA interference. Proc. Natl. Acad. Sci. USA *101*, 4912–4917.

Sedding, D. G., Hermsen, J., Seay, U., Eickelberg, O., Kummer, W., Schwencke, C., Strasser, R. H., Tillmanns, H., and Braun-Dullaeus, R. C. (2005). Caveolin-1 facilitates mechanosensitive protein kinase B (Akt) signaling in vitro and in vivo. Circ. Res. *96*, 635–642.

Shaklee, P. M., Idema, T., Koster, G., Storm, C., Schmidt, T., and Dogterom, M. (2008). Bidirectional membrane tube dynamics driven by nonprocessive motors. Proc. Natl. Acad. Sci USA *105*, 7993–7997.

Shao, Y., Akmentin, W., Toledo-Aral, J. J., Rosenbaum, J., Valdez, G., Cabot, J. B., Hilbush, B. S., and Halegoua, S. (2002). Pincher, a pinocytic chaperone for nerve growth factor/TrkA signaling endosomes. J. Cell Biol. *157*, 679–691.

Sharma, D. K., Brown, J. C., Choudhury, A., Peterson, T. E., Holicky, E., Marks, D. L., Simari, R., Parton, R. G., and Pagano, R. E. (2004). Selective stimulation of caveolar endocytosis by glycosphingolipids and cholesterol. Mol. Biol. Cell *15*, 3114–3122.

Sharma, D. K., Choudhury, A., Singh, R. D., Wheatley, C. L., Marks, D. L., and Pagano, R. E. (2003). Glycosphingolipids internalized via caveolar-related endocytosis rapidly merge with the clathrin pathway in early endosomes and form microdomains for recycling. J. Biol. Chem. *278*, 7564–7572.

Shibata, Y., Voss, C., Rist, J. M., Hu, J., Rapoport, T. A., Prinz, W. A., and Voeltz, G. K. (2008). The reticulon and Dp1/Yop1p proteins form immobile oligomers in the tubular endoplasmic reticulum. J. Biol. Chem. *283*, 18892–18904.

Shnyrova, A., Frolov, V. A., and Zimmerberg, J. (2008). ER biogenesis: self-assembly of tubular topology by protein hairpins. Curr. Biol. *18*, R474–R476.

Sloan, E. K., Stanley, K. L., and Anderson, R. L. (2004). Caveolin-1 inhibits breast cancer growth and metastasis. Oncogene *23*, 7893–7897.

Smirnova, E., Goldberg, E. B., Makarova, K. S., Lin, L., Brown, W. J., and Jackson, C. L. (2006). ATGL has a key role in lipid droplet/adiposome degradation in mammalian cells. EMBO Rep. *7*, 106–113.

Sun, X.-H., Flynn, D. C., Castranova, V., Millecchia, L. L., Beardsley, A. R., and Liu, J. (2007). Identification of a novel domain at the N terminus of caveolin-1 that controls rear polarization of the protein and caveolae formation. J. Biol. Chem. *282*, 7232–7241.

Tagawa, A., Mezzacasa, A., Hayer, A., Longatti, A., Pelkmans, L., and Helenius, A. (2005). Assembly and trafficking of caveolar domains in the cell: caveolae as stable, cargo-triggered, vesicular transporters. J. Cell Biol. *170*, 769–779.

Thomsen, P., Roepstorff, K., Stahlhut, M., and van Deurs, B. (2002). Caveolae are highly immobile plasma membrane microdomains, which are not involved in constitutive endocytic trafficking. Mol. Biol. Cell *13*, 238–250.

Várnai, P., and Balla, T. (1998). Visualization of phosphoinositides that bind pleckstrin homology domains: calcium- and agonist-induced dynamic changes and relationship to myo-[3H]inositol-labeled phosphoinositide pools. J. Cell Biol. *143*, 501–510.

Vogel, V., and Sheetz, M. P. (2009). Cell fate regulation by coupling mechanical cycles to biochemical signaling pathways. Curr. Opin. Cell Biol. *21*, 38–46.

Volpicelli, L. A., Lah, J. J., and Levey, A. I. (2001). Rab5-dependent trafficking of the m4 muscarinic acetylcholine receptor to the plasma membrane, early endosomes, and multivesicular bodies. J. Biol. Chem. *276*, 47590–47598.

Wei, Q., and Adelstein, R. S. (2000). Conditional expression of a truncated fragment of nonmuscle myosin II-A alters cell shape but not cytokinesis in HeLa cells. Mol. Biol. Cell *11*, 3617–3627.

Wiechen, K., *et al*. (2001a). Caveolin-1 is down-regulated in human ovarian carcinoma and acts as a candidate tumor suppressor gene. Am. J. Pathol. *159*, 1635–1643.

Wiechen, K., Sers, C., Agoulnik, A., Arlt, K., Dietel, M., Schlag, P. M., and Schneider, U. (2001b). Down-regulation of caveolin-1, a candidate tumor suppressor gene, in sarcomas. Am. J. Pathol. *158*, 833–839.

Williams, T. M., and Lisanti, M. P. (2005). Caveolin-1 in oncogenic transformation, cancer, and metastasis. Am. J. Physiol. Cell Physiol. *288*, C494–C506.

Yu, J., Bergaya, S., Murata, T., Alp, I. F., Bauer, M. P., Lin, M. I., Drab, M., Kurzchalia, T. V., Stan, R. V., and Sessa, W. C. (2006). Direct evidence for the role of caveolin-1 and caveolae in mechanotransduction and remodeling of blood vessels. J. Clin. Invest. *116*, 1284–1291.